

Exploring Gradient Subspaces: Addressing and Overcoming LoRA's Limitations in Federated Fine-Tuning of Large Language Models

Navyansh Mahla¹, Kshitij Sharad Jadhav¹, Ganesh Ramakrishnan¹

¹Indian Institute of Technology Bombay

210040106@iitb.ac.in, kshitij.jadhav@iitb.ac.in, ganesh@cse.iitb.ac.in

Abstract

Large Language Models (LLMs) have demonstrated remarkable capabilities across various domains, particularly in task generalization for both text and vision data. While fine-tuning these models can significantly enhance their performance on specific downstream tasks, it often requires high-quality data that cannot be shared due to privacy concerns. Federated Learning (FL) offers a promising solution for collaborative training without direct data sharing. However, many parameter-efficient fine-tuning strategies for LLMs in FL, particularly those based on Low-Rank Adaptation (LoRA), face limitations. In this paper, we critically analyze the convergence and performance guarantees of popular FL frameworks utilizing LoRA, highlighting its suboptimal nature due to constrained subspace learning of low-rank matrices. This limitation hinders effective fine-tuning of LLMs in federated settings. Through rigorous analytical and empirical evaluations, we demonstrate that direct weight averaging outperforms LoRA-based strategies, leading to superior performance for fine-tuned models. Our comprehensive comparison unmasks inefficiencies in LoRA approaches and underscores the advantages of direct weight aggregation. We extend our analysis to low-rank gradient-based optimizers, such as GaLore, used during local training steps. Our findings show that GaLore along with direct-weight aggregation is a more effective approach, outperforming federated LoRA methods like FlexLoRA and FFA-LoRA across both text and image modalities. While privacy remains paramount in FL discourse, our focus is on assessing performance outcomes of federated fine-tuned models and evaluating various FL frameworks from both theoretical and empirical perspectives. Our findings advocate reassessing the reliance on LoRA within FL contexts, paving the way for more efficient training methodologies.

Introduction

The past few years have witnessed unprecedented advancements in Large Language Models (LLMs) (Brown et al. 2020; OpenAI 2023; Du et al. 2024; Touvron et al. 2023; Zeng et al. 2022; Zhang et al. 2022). These language models (LMs) are powered by Transformer (Vaswani et al. 2017) neural network architecture. Since the transformer models have extensive pre-trained context, they exhibit enhanced generalization capabilities, providing them effective few-

shot learning capabilities (Brown et al. 2020). The introduction of Vision Transformers (ViTs) (Dosovitskiy et al. 2021) has extended the capabilities of transformers to process image modalities. Like their counterparts in language processing, ViTs are pre-trained on vast image datasets, enabling them to achieve a robust contextual understanding of visual content. Models such as CLIP (Contrastive Learning Image Pre-training) (Radford et al. 2021a) have facilitated the integration of text and image modalities by aligning their representations into a shared subspace. This has led to the development of Vision-Language Models (VLMs) and Large Multimodal Model (LMM) (Liu et al. 2023) architectures, enabling transformer networks to interpret and reason over text and image prompts simultaneously, thereby enhancing their capabilities in visual question answering. These pre-trained language models can be further fine-tuned to improve performance on specific downstream tasks (Radford et al. 2021a). However, the good-quality datasets required for fine-tuning can be distributed and may not be shared directly due to privacy concerns. Researchers have turned to Federated Learning (FL) (McMahan et al. 2017) as a means to fine-tune LLMs without compromising the data privacy (Qin et al. 2024; Zhang et al. 2024a; Bai et al. 2024; Babakniya et al. 2023). In these settings, parameter-efficient fine-tuning methods (Ding et al. 2023) like LoRA (Hu et al. 2022) are utilized to minimize computational overhead. We analyze the most recent SOTA LoRA approaches, which include FlexLoRA (Bai et al. 2024) and FFA-LoRA (Sun et al. 2024b), and identify potential bottlenecks resulting in their performance degradation.

We demonstrate that the direct weight aggregation strategy effectively addresses the limitations of LoRA in federated learning contexts to some extent. Building on this analysis, we theoretically establish that gradient low-rank optimizers, such as GaLore (Zhao et al. 2024) coupled with direct weight averaging, represent a more effective fine-tuning approach for both large language models (LLMs) and vision transformers (ViTs) in federated settings. Our theoretical insights are validated through experiments that reveal the suboptimal performance of LoRA-based methods in FL environments. Notably, combining direct weight aggregation with GaLore as an optimizer for local training steps significantly outperforms leading state-of-the-art LoRA methods like FlexLoRA and FFA-LoRA. We list the contributions of

our paper below:

- We highlight the sub-optimal nature of the most recent LoRA-based SOTA methods like FlexLoRA (Bai et al. 2024) and FFA-LoRA (Sun et al. 2024b) in FL.
- We provide analytical evidence that LLMs and ViTs fine-tuned with the GaLore optimizer during local training, when directly aggregated with FedAvg, outperform methods like LoRA. Our study demonstrates this through a straightforward experimental setup using the GaLore optimizer for parameter updates and direct weight aggregation using FedAvg.
- We present results on text and image modalities using vision and language transformers across multiple clients and configurations, surpassing current SOTA LoRA methods and validating our theoretical analysis of LoRA’s sub-optimality.

Related Works

Parameter Efficient Fine-Tuning of LLMs

Pre-trained transformers, trained on extensive text or image datasets, gain broad contextual understanding. Fine-tuning these models improves their performance on targeted downstream tasks (Radford et al. 2021b). However, fine-tuning on consumer-grade GPUs is challenging due to their large parameter count, which demands significant GPU memory. To address this computational complexity, researchers have proposed Parameter Efficient Fine-Tuning (PEFT) (Ding et al. 2023) techniques like prompt tuning (Lester, Al-Rfou, and Constant 2021), adapter tuning (He et al. 2021; Houlsby et al. 2019), and Low-Rank Adaptation (LoRA) (Hu et al. 2022). Adapter learning techniques add trainable parameters to the model sequentially while keeping other components frozen. This reduces the overall number of trainable parameters, enabling fine-tuning on smaller GPUs. In LoRA, adapters are applied in parallel and decomposed into lower-rank matrices, further optimizing parameter efficiency. Similarly, prefix and prompt tuning involve applying modules in parallel to attention heads (Li and Liang 2021) or embeddings (Lester, Al-Rfou, and Constant 2021) to achieve efficient fine-tuning. The model’s fine-tuning performance greatly depends on the dataset’s size and quality (Sun et al. 2024a). Good-quality datasets are often distributed across multiple parties, as a single source may be insufficient for effective fine-tuning. Privacy concerns and regulations like the General Data Protection Regulation (GDPR) further prevent centralizing data for collaborative efforts, especially under the new EU Act (Woisetschläger et al. 2024).

PEFT in Federated Learning

Federated Learning (FL) (McMahan et al. 2017) addresses this issue by enabling collaborative neural network training without data centralization. It has been successfully applied to various architectures, including transformers (Bai et al. 2024; Qin et al. 2024; Zhang et al. 2024a; Babakniya et al. 2023; Kuang et al. 2023; Cho et al. 2023; Ansell et al. 2022; Alam et al. 2022; Niu et al. 2022; Diao, Ding, and Tarokh

2021). However, the massive size of large language models demands substantial resources for inter-client communication and local training, highlighting the need for more compute and communication-efficient paradigms in FL fine-tuning. Due to their efficiency in fine-tuning, PEFT approaches are well-suited for FL schemes to solve such problems. LoRA has been prominently utilized in fine-tuning language models in FL settings as discussed in several studies (Bai et al. 2024; Qin et al. 2024; Zhang et al. 2024a; Cho et al. 2023; Kuang et al. 2023; Babakniya et al. 2023). Many of these studies adopt FedAvg (McMahan et al. 2017) as the aggregation algorithm to aggregate client-side parameters onto a server model. For instance, FedIT (Zhang et al. 2024a) fine-tunes models in decentralized settings by sharing and aggregating LoRA matrices (let B be the zero-initialized LoRA matrix and A be the Gaussian initialized LoRA matrix) separately. SLoRA (Babakniya et al. 2023) introduces a two-stage sparse fine-tuning approach with improved LoRA matrix initialization for federated learning. Following the improved initialization, a mechanism similar to that of FedIT is adopted for distributed training. FlexLoRA (Bai et al. 2024) enhances previous methods by allowing diverse LoRA weight mixtures across clients, claiming superior performance compared to SLoRA in homogeneous settings and HETLORA (Cho et al. 2023) in heterogeneous settings. Instead of aggregating LoRA matrices separately, FlexLoRA multiplies matrices B and A before aggregation, then decomposes the resulting matrix into low-rank components via truncated SVD, with the decomposed matrices copied to the LoRA matrices B and A of each client. Other strategies, such as FFA-LoRA (Sun et al. 2024b), focus on fine-tuning only matrix B while keeping all other parameters frozen across varying tasks, hyperparameters, and privacy protection levels. In contrast, our approach FedFTG only fine-tunes the MLP layers without any adapters with GaLore (Zhao et al. 2024) optimization to reduce memory usage for optimization states.

Galore in LLMs and ViTs

Galore is a subspace gradient learning approach designed for memory-efficient training of LLMs. This method reduces the memory footprint of optimizer states by projecting gradient matrices into a low-rank subspace before applying optimization techniques such as AdamW (Loshchilov and Hutter 2019) or SGD (Ruder 2017). Recent studies, such as MedSAGa (Mahla et al. 2024), have empirically validated Galore’s effectiveness for tasks like image segmentation. Authors fine-tuned ViT-based Segment Anything Model (SAM) (Kirillov et al. 2023) using Galore, showcasing its applicability beyond traditional language modeling tasks.

Methodology

Problem Setting

We frame our problem within a multi-silo environment where each silo (client) hosts the same Large Language Model (LLM) M to fine-tune along with a dataset $\mathcal{D}_i = \{(x_j^i, y_j^i)\}_{j=1}^n\}$ (assuming all the N clients have the same

sample size n) that is non-independent and identically distributed (non-IID) compared to datasets of other clients. \mathcal{D}_i^T and \mathcal{D}_i^E respectively represent the train and eval split of the dataset \mathcal{D}_i . A single server facilitates the global aggregation of client parameters of N clients. Due to privacy concerns, these clients cannot share the data with the server for centralized training. $\theta_i \forall t \in \{1, 2, \dots, N\}$ are the model parameters at client i and θ_g are the model parameters at the server. We define the distributed learning objective as:

$$\min_{\theta_g} \frac{1}{N} \sum_{i=1}^N \left(\mathcal{L}_i(\theta_g) := \mathbb{E}_{(x,y) \in \mathcal{D}_i^E} l(M(x; \theta_g), y) \right) \quad (1)$$

Where l is the convex loss function. Each client performs its own local training step:

$$\mathcal{L}_i(\theta_i) = \frac{1}{|\mathcal{D}_i^T|} \sum_{(x,y) \in \mathcal{D}_i^T} l(M(x; \theta_i), y) \quad (2)$$

After some local iterations T_{agg} , the parameters are sent to the server for aggregation using FedAvg:

$$\theta_g := \frac{1}{|\mathcal{D}|} \sum_{i=1}^N |\mathcal{D}_i^T| \theta_i$$

Here, $|\mathcal{D}|$ is the sum of the size of the train split of the datasets of all the clients. These aggregated parameters are subsequently copied back to each client model to resume training. This allows local iterations to proceed with the model parameters θ_g , which were aggregated during the latest global aggregation step.

Why Not LoRA?

In this section, we analyze the use of LoRA in FL from the perspective of two of the most recent SOTA LoRA FL schemes: FlexLoRA (Bai et al. 2024) and FFA-LoRA (Sun et al. 2024b). Both of these methods have presented their own analysis of the vanilla LoRA FL scheme FedIT (Zhang et al. 2024a). The authors of FlexLoRA question LoRA's efficiency in highly heterogeneous tasks across different clients. They discuss the infeasibility of existing LoRA solutions like FedIT in FL settings due to the *bucket effect* caused by different intrinsic ranks at each client because of heterogeneous datasets. On the other hand, authors of FFA-LoRA perform a rigorous analysis of vanilla LoRA method like FedIT in the "client-drift" (Karimireddy et al. 2020) scenario and the amplification of noise in FL settings with DP-SGD (Abadi et al. 2016) due to semi-quadratic structure of LoRA. With thorough analysis, both of these methods were able to outperform vanilla LoRA FL method. Here, we present our analysis of why the SOTA LoRA frameworks like FlexLoRA and FFA-LoRA are sub-optimal under multi-client FL settings.

The core idea of LoRA is to constrain the weight update on the model by a low-rank decomposition:

$$\mathbf{W}_0 + \Delta \mathbf{W} = \mathbf{W}_0 + \mathbf{B} \mathbf{A} \quad (3)$$

Here $\mathbf{W}_0 \in \mathbb{R}^{d \times k}$ is the pre-trained weight matrix which is frozen during the training process. Updates are performed on

$\mathbf{A} \in \mathbb{R}^{r \times k}$ and $\mathbf{B} \in \mathbb{R}^{d \times r}$. \mathbf{B} is initialized as zero while \mathbf{A} uses random Gaussian initialization. Here, $r \ll \min(d, k)$. This reduces the number of training parameters by a factor of $\frac{d \times k}{r \times (k+d)}$ compared to full parameter fine-tuning.

Proposition 1 *In FL scenarios like FlexLoRA, where parameter change matrices $\Delta \mathbf{W}_i$ from N clients are aggregated with each client i having an intrinsic rank r_i , the globally aggregated parameter matrix exhibits rank inflation following each global aggregation step. Specifically, in a scenario where all clients have identical ranks $r_i = r$ for simplicity, the rate of rank inflation, denoted by η satisfies $1 \leq \eta \leq N$ per global aggregation step.*

The equality on the left holds true when the ranks of all matrices share the same subspace, a condition that becomes unattainable when data samples are non-IID across clients. Further details, including the proof of this proposition and a more comprehensive discussion, are available in the supplementary material.

In FlexLoRA, the LoRA matrices \mathbf{B} and \mathbf{A} are multiplied and then aggregated across clients. The product of these matrices is then subjected to Singular Value Decomposition (SVD) to decompose it back to the original LoRA rank. However, this approach faces a significant challenge: after aggregation, the resulting rank of the matrix is inflated (as shown in Proposition 1), capturing more comprehensive information from all the non-IID datasets. When this aggregated matrix is reduced to a smaller dimension via SVD, it consistently maps the weights to a subspace of fixed rank—the same as the LoRA rank, which remains constant throughout training. This dimensionality reduction can create a bottleneck, as it restricts the model's ability to efficiently capture and leverage the learned local semantics from non-IID datasets. By decomposing the weights into ranks smaller than the actual rank of the aggregated matrix, valuable information may be lost, thereby limiting the effectiveness of FlexLoRA in federated learning scenarios with diverse data distributions.

For fine-tuning LLMs in FL settings using FFA-LoRA:

$$\Delta \mathbf{W}_{agg} = \frac{1}{N} \sum_{i=1}^N \Delta \mathbf{W}_i = \frac{1}{N} \sum_{i=1}^N \Delta \mathbf{B}_i \mathbf{A}_0 \quad (4)$$

The Gaussian initialized LoRA matrix \mathbf{A} is frozen for all the clients. Essentially, aggregation happens for the zero initialized LoRA matrices $\mathbf{B}_i \forall i \in \{1, 2, \dots, N\}$.

Theorem 1 *For a convex loss \mathcal{L} , let $\Delta \mathbf{W}^* \in \mathbb{R}^{d \times k}$ be the optimal LoRA parameter matrix, α be the learning rate and $\mathbf{A}_0 \in \mathbb{R}^{r \times k}$ be a Gaussian initialized random matrix, where $r \ll \min(d, k)$ and the L2 norm of the gradient to be bounded (i.e. $\|\nabla_{\mathbf{W}} \mathcal{L}^{(i)}(\Delta \mathbf{W})\|_2 \leq D$). The excess risk ($|\mathcal{L}(\Delta \mathbf{W}_{agg}) - \mathcal{L}(\Delta \mathbf{W}^*)|$) bounds for the FFA-LoRA framework, involving N clients and S global aggregation steps having occurred every t_{agg} local training iterations, can be expressed as follows:*

$$\begin{aligned} &\leq DNSt_{agg} \left(DNSt_{agg}c + \frac{\alpha}{N} \|\Delta \mathbf{W}^*\|_2 \right) \\ &= \mathcal{O}(N^2 S^2 t_{agg}^2) \end{aligned} \quad (5)$$

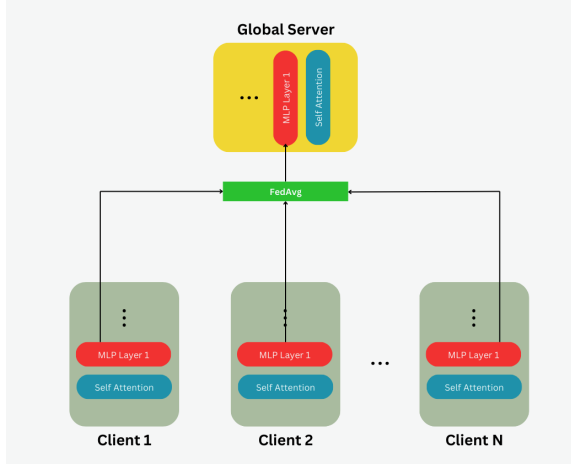


Figure 1: FedFTG exclusively fine-tunes the lower MLP layers of the transformer network while keeping all other components frozen. GaLore is used as an optimizer, and similar to standard federated learning setups, globally aggregated parameters are copied back to each client after each global aggregation round.

Here, $\Delta\mathbf{W}^*$ is hypothetically the most optimal LoRA adapter matrix and c is a constant scalar.

Theorem 1 is crucial to our analysis as it demonstrates that the excess risk bounds for FFA-LoRA are upper-bounded by an expression that increases with each FedAvg global aggregation step S . This indicates that models trained using the FFA-LoRA framework progressively deviate from the optimal hypothesis as the number of FedAvg steps increases, leading to instability. Consequently, due to this divergence, the model struggles to capture the overall data distribution across all clients, resulting in poor generalization over unseen data samples. We refer to the supplementary material for the proofs and detailed discussions on the theorem.

How can we improve?

The previous section offers valuable insights into the sub-optimal behavior of LoRA in federated settings. In particular, the use of low-rank adapters hinders efficient learning, as the low-rank subspace expands with each global FedAvg aggregation step. This is particularly suboptimal for FlexLoRA, while for FFA-LoRA, the bounds on excess risk are quadratic. Therefore, we recommend against using low-rank adapters. Instead, we advocate for the direct averaging of parameters in federated settings. Direct weight aggregation in itself poses problems such as computational inefficiency. LoRA is a parameter efficient approach which results saving a lot of compute. Direct weight averaging won't be parameter efficient. To optimize memory usage and enable all clients to fine-tune LLMs locally, we recommend using GaLore as the optimizer during local training iterations. GaLore is an optimization method that improves memory efficiency while training of transformer based models (Zhao et al. 2024). GaLore reduces optimizer state memory usage by projecting weight gradients onto a lower-dimensional

subspace, where the optimization process is then carried out. Interestingly, this approach not only saves memory but also leads to linear excess risk bounds, as demonstrated in the following theorem:

Theorem 2 For a convex loss function \mathcal{L} , let $\Delta\mathbf{W}^*$ denote the optimal weight matrix and α represent the learning rate. Assuming that the L_2 norm of the gradient is bounded, specifically $\|\nabla_{\mathbf{W}} \mathcal{L}^{(i)}(\Delta\mathbf{W})\|_2 \leq D$, the excess risk, defined as $|\mathcal{L}(\Delta\mathbf{W}_{agg}) - \mathcal{L}(\Delta\mathbf{W}^*)|$, for the aggregated weights after a total of S direct FedAvg aggregations having occurred every t_{agg} local training iterations with GaLore as an optimizer can be expressed as follows:

$$|\mathcal{L}(\Delta\mathbf{W}_{agg}) - \mathcal{L}(\Delta\mathbf{W}^*)| \leq \alpha D^2 S t_{agg} + c = \mathcal{O}(S t_{agg}) \quad (6)$$

Here, c is a scalar constant.

Concluding from theorem 2, the upper bounds on excess risk for direct weight averaging are independent of the number of clients and exhibit a linear relationship (contrary to quadratic in case of LoRA (theorem 1)) with the number of global FedAvg steps and local training iterations t_{agg} . Adopting direct weight averaging with GaLore as an optimizer for fine-tuning in federated settings ensures that excess risk remains unaffected by client count. This trend is further supported by the experimental results presented in later sections. We will use FedAvg as the global aggregation algorithm, as it is widely used in federated fine-tuning for large language models. Combining FedAvg with direct weight averaging allows for a fair comparison and shows that even a simple algorithm like FedAvg can yield significantly better results when paired with a more efficient framework. In the context of transformer neural networks, the GaLore paper demonstrates that the low-rank projection of gradient matrices can be effectively applied to its lower MLP layers like *project-up* (see Lemma B.6 from GaLore paper) whose gradients become low-rank during training. Consequently, unless stated otherwise, we conduct all our analyses and experiments on the lower MLP layers. Another advantage of using GaLore is its improved generalization error compared to LoRA-based methods, as demonstrated by the following theorem (None of the theorems assume a specific client dataset size; they account for both equal and different dataset sizes):

Theorem 3 Let N denote the number of clients, each possessing a dataset with n samples. We consider the weights of a lower-level MLP layer represented by $\mathbf{W} \in \mathbb{R}^{d \times k}$. Under the assumption that the risk function of each client is σ -sub-Gaussian with respect to the data distribution of that client and the corresponding weight matrix, we derive the following generalization error bounds for weight aggregation:

a) For federated fine-tuning using FFA-LoRA:

$$\mathcal{E}_1 \leq \frac{1}{N} \sum_{i=1}^N \sqrt{\frac{2\sigma^2 \ln 2}{n} r q \sum_i (d)} \quad (7)$$

b) or direct weight aggregation using FedAvg with a low-

rank gradient-based optimizer, such as *GaLore*:

$$\mathcal{E}_2 \leq \frac{1}{N} \sum_{i=1}^N \sqrt{-\frac{2\sigma^2}{n} \sum_{j=1}^d \sum_{l=1}^k f(\mathbf{W}_i^{(j)}[l], t) \log(f(\mathbf{W}_i^{(j)}[l], t))} \quad (8)$$

where $\mathbf{W}_i^{(j)}[l]$ represents the element of l th index in the j th row of the matrix \mathbf{W}_i . Here, $f(\mathbf{W}_i^{(j)}[l], t) = \frac{\exp(\mathbf{W}_i^{(j)}[l])}{\sum_{l=1}^k \exp(\mathbf{W}_i^{(j)}[l])}$ be the function to represent the ratio (probability) in a succinct manner. As $t \rightarrow \infty$, i.e. as the federated training continues $f(\mathbf{W}_i^{(j)}[l], t) \rightarrow \frac{1}{k}$.

As one can infer from the theorem, generalization error \mathcal{E}_2 at the end of the training becomes upper bounded by $\frac{1}{N} \sum_{i=1}^N \sqrt{\frac{2\sigma^2 d}{nk} \log k}$ which is much smaller than that of the part (a) ($\mathcal{E}_1 \leq \frac{1}{N} \sum_{i=1}^N \sqrt{\frac{2\sigma^2 \ln 2}{n} r q d}$). Thus, direct averaging with *GaLore* optimizer shows better generalization than FFA-LoRA framework. Notably, overall entropy decreases during *GaLore*-based direct FedAvg aggregation, indicating more structured weight matrices, which correlates with enhanced generalization performance. Integrating the *GaLore* optimizer with FedAvg effectively leads to rank reduction (considering fixed quantization bits q), confining the learning process to a compact, structured subspace with lower entropy. This localized learning is important as it achieves comparable excess risk bounds while operating in a reduced parameter space, enhancing computational efficiency. Our analysis shows salient feature learning in federated settings similar to (Tian et al. 2024) which is for centralized cases. The framework focuses on learning shared salient features across distributed datasets, creating a common subspace that facilitates effective performance across all client distributions. As training advances, the parameter matrix converges to a well-defined, approximately linear manifold due to the reduced rank. The gradient matrix exhibits similar low-rank behavior as $t \rightarrow \infty$, suggesting it also manifests on a near-linear manifold. *GaLore* integration in federated learning outperforms traditional LoRA-based weight averaging through better efficiency, better risk bounds, and stronger generalization guarantees. This leads us to explore optimal ways to implement *GaLore* for distributed fine-tuning to maximize its subspace learning benefits. To address this challenge, we introduce **FedFTG** (Federated Fine Tuning using *GaLore*), an experimental framework for federated learning that is designed for federated fine-tuning scenarios while using *GaLore* for local training steps at each client.

Federated Fine-Tuning Using *GaLore* (FedFTG)

In previous sections, we highlighted the limitations of low-rank adapter tuning for LLMs in federated settings. We also demonstrated that using *GaLore* as an optimizer for local training offers superior generalization, improved memory efficiency, and better training performance overall. We refer to the JoMA paper (Tian et al. 2024) (Theorem 1 of the paper) that states that we do not need to explicitly update the self-attention parameters since it is already implicitly incorporated in the lower layer of MLP weight. Consequently,

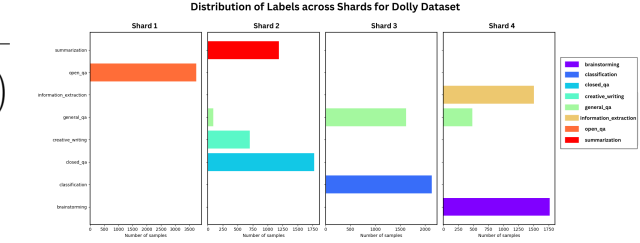


Figure 2: Label distribution across shards for the Dolly dataset produced using Dirichlet Allocation with $\alpha = 0.1$.

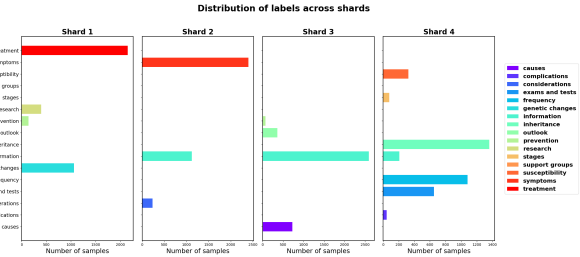


Figure 3: Label distribution across shards for the MedQuAD dataset produced using Dirichlet Allocation with $\alpha = 0.1$.

we focus on fine-tuning the lower MLP layers (*project-up*) of the transformer neural network. This is consistent with Theorem 3, which addresses the scenario where the lower MLP layers are fine-tuned. Since the self-attention information is inherently captured within these lower MLP layers, and these layers typically exhibit lower generalization error in federated settings, we recommend focusing on fine-tuning only the lower MLP layers. To update the parameters in FedFTG, we utilize *GaLore*, as detailed in the previous section. The entire pipeline is shown in the figure 1. The complete FedFTG algorithm pipeline is detailed in the accompanying algorithm. FedFTG is an experimental setup that validates our theory against current SoTA LoRA approaches, addressing their low-rank learning constraints and training stability issues.

Experiments

In this section, we demonstrate the stability and efficiency of models trained with *GaLore* as the optimizer and direct weight aggregation. We evaluate its performance across both text and image modalities to showcase its effectiveness on LLMs and ViTs. For the text modality, experiments involve 3 and 4 clients, while vision experiments include 3, 4, and 5 clients, with each client hosting a non-IID dataset distinct from others. All experiments were conducted on a cluster of Nvidia A6000 GPUs, with setup details provided in the supplementary material.

Datasets

We conduct experiments on both text and image datasets, incorporating various downstream tasks. For text, we use the MedQuAD (Ben Abacha and Demner-Fushman 2019)

Algorithm 1: FedFTG

Input: Model \mathcal{M} from each client i with non-IID datasets $\mathcal{D}_i = \{(x_j^i, y_j^i)\}_{j=1}^n$, learning rates η_i

Parameter: Client parameters θ_i , global parameters θ_g , aggregation period T_{agg} , total mini-batches T

Output: Optimized global parameters θ_g after e epochs

```

1: Initialize  $\theta_g$ 
2: for epoch = 1, ...,  $e$  do
3:   Initialize all local  $\theta_i \leftarrow \theta_g$  in parallel
4:   for  $t = 1, \dots, T$  do
5:     for all client  $i \in \{1, \dots, N\}$  in parallel do
6:       Sample mini-batch  $\mathcal{B}_i$  from  $\mathcal{D}_i$ 
7:        $G(\theta_i, \mathcal{B}_i) \leftarrow \nabla_{\theta_i} \mathcal{L}(\mathcal{M}(\theta_i; \mathcal{B}_i), \mathcal{B}_i)$ 
8:        $\theta_i \leftarrow \theta_i - \eta_i \text{GaLore}(G(\theta_i, \mathcal{B}_i))$ 
9:     end for
10:    if  $t \bmod T_{agg} = 0$  then
11:       $\theta_g \leftarrow \frac{1}{N} \sum_{i=1}^N \theta_i$ 
12:      Update all local  $\theta_i \leftarrow \theta_g$  in parallel
13:    end if
14:  end for
15: end for
16: return  $\theta_g$ 

```

and Databricks Dolly 15k (Conover et al. 2023) datasets. MedQuAD is a medical question-answering dataset containing 47,457 question-answer pairs sourced from 12 NIH websites, covering 39 question types related to diseases, drugs, and other medical entities. However, owing to the MedlinePlus copyright, answers from the 3 subsets were removed. Databricks Dolly-15k contains 15,000 high-quality human-generated prompt/response pairs designed for instruction tuning LLMs. It includes various categories like brainstorming, classification, summarization, and question answering. For experiments related to vision modality, we utilize the Brain Tumour classification dataset (Cheng 2017) which comprises of 3,064 T1-weighted contrast-enhanced MRI images from 233 patients, categorized into three tumor types: meningioma (708 slices), glioma (1,426 slices), and pituitary tumor (930 slices). The task is to identify the correct tumor type by having the MRI image fed as an input to the ViT. More details on these datasets are discussed in the data appendix of the supplementary material.

Non-IID Data Preparation

To simulate non-IID conditions, we used Dirichlet Allocation to partition each dataset into several non-IID splits similar to (Zhang et al. 2024a; Hsu, Qi, and Brown 2019). For the text datasets (MedQuAD and Dolly 15k), we generated 4 splits, whereas for the Brain Tumor Classification dataset, we created 5 splits. The concentration parameter α was set to 0.1, resulting in highly skewed distributions across clients that replicate non-IID behavior in FL settings. Splits are created based on labels. For MedQuAD dataset, the label is *question_type* while for Dolly-15k it is *category*. The shards prepared for a given dataset are of the same sizes. Class la-

bel distribution across each non-IID shard for all the datasets (both image and text) can be found in the supplementary material.

Models and Hyperparameters

For experiments on text datasets (MedQuAD and Dolly-15k), we utilize Gemma-2B (Team et al. 2024) and TinyLlama (Zhang et al. 2024b). In FedFTG, we fine-tuned the *up-proj* MLP layer, which follows the self-attention module. Conversely, FlexLoRA and FFA-LoRA focused on fine-tuning the attention modules (query, key, value) with a LoRA rank of 8 and a scaling factor of 16, in line with the experimental setups presented in their original papers. For vision modality experiments, we fine-tuned SigLIP (Zhai et al. 2023). In FedFTG applied to SigLIP, we fine-tuned the MLP layer immediately after the attention module and the classifier layer (see supplementary material for more details). FlexLoRA and FFA-LoRA, on the other hand, fine-tuned the attention parameters (query, key, value) with a LoRA rank of 8 similar to text experiments and a scaling factor of 32.

Training and Evaluation

We conducted our experiments with different numbers of clients. For text datasets, we evaluated FedFTG with 3 and 4 clients. With 3 clients, shards 1, 2, and 3 of each dataset were used, while with 4 clients, all shards were utilized. A similar shard assignment was used for the Brain Tumour Classification dataset. Each shard was split into training and test sets, with 1% of samples reserved for testing in the text datasets and 5% for the vision dataset (vision dataset shards are much smaller thus larger fraction of test set is required for making a firm conclusion). The global evaluation set was created by combining the test sets from each shard, thus containing unseen samples from different non-IID shards. This helps assess the model’s generalization ability in distributed non-IID settings. Text datasets were trained with a batch size of 1, while the image dataset used a batch size of 2, with all models trained for 3 epochs.

Experiment Results

Table 1 shows the results on text datasets. We report the ROUGE_L F1 (Longest common subsequence ROUGE) score (Lin 2004) and the BLEU-4 (4-gram) (Papineni et al. 2002) score for text datasets. Out of 3 epochs, we report the results of the epoch which has the best result. This is done owing to the overfitting of models usually in some experiment runs. Table 1 shows that FedFTG consistently surpasses both FlexLoRA and FFA-LoRA across different numbers of clients and datasets. Table 2 shows the results of fine-tuning SigLIP on the Brain Tumor Classification Dataset for tumor type classification. In this vision dataset experiment, FedFTG outperforms both LoRA-based FL methods. The notably poorer performance of FFA-LoRA across text and vision experiments aligns with earlier analyses, as its excess risk bounds increase with each FedAvg step (Theorem 1), hindering efficient learning of the dataset’s semantics and leading to suboptimal results. Figure 8 displays the variation in ROUGE_L F1 scores on the global evaluation set across FedAvg steps for TinyLlama, with similar

N	Dataset	Model	Method	BLEU-4	ROUGE-L
3	MedQuAD	TinyLlama	FedFTG	0.4883	0.6637
			FlexLoRA	0.4551	0.6429
			FFA-LoRA	0.1004	0.2947
	Dolly-15K	Gemma-2B	FedFTG	0.5493	0.7019
			FlexLoRA	0.4238	0.6401
			FFA-LoRA	0.1077	0.2875
4	MedQuAD	TinyLlama	FedFTG	0.3157	0.5244
			FlexLoRA	0.2873	0.5221
			FFA-LoRA	0.0566	0.1708
	Dolly-15K	Gemma-2B	FedFTG	0.3284	0.5413
			FlexLoRA	0.2874	0.5375
			FFA-LoRA	0.1077	0.2875

Table 1: Comparison of BLEU-4 and ROUGE L F1 scores across different methods, models, and datasets for varying client numbers with non-IID splits

graphs for the Gemma-2B model in the supplementary material. FFA-LoRA’s ineffective aggregation, shown at the bottom of the graphs, shows minimal improvements with more FedAvg steps. While FlexLoRA experiences performance dips on the MedQuAD dataset, it still achieves reasonable aggregation efficiency but falls short compared to FedFTG. In contrast, FedFTG demonstrates the most stable aggregation results, maintaining consistent training performance without abrupt drops. Overall, FedFTG outperforms both FlexLoRA and FFA-LoRA across various clients, datasets, and downstream tasks (Table 1 and 2).

The supplementary material includes more detailed explanation of the results and additional experiments with varying label distributions. Across these configurations, FedFTG consistently outperforms FlexLoRA and FFA-LoRA, with results validated over two independent runs, reinforcing our findings.

Conclusion and Future Work

Our analysis begins by examining LoRA’s performance in federated settings, focusing on state-of-the-art frameworks FlexLoRA and FFA-LoRA, with particular attention to constraints imposed by low-rank adapter subspace learning. This investigation extends to direct weight aggregation methods and the application of GaLore as an optimization strategy, where we provide theoretical insights demonstrating its advantages over LoRA-based approaches. We introduce FedFTG, a streamlined approach for fine-tuning

No of clients	Method	F1 Score
3	FedFTG	0.6064
	FlexLoRA	0.5638
	FFA-LoRA	0.0165
4	FedFTG	0.843
	FlexLoRA	0.4868
	FFA-LoRA	0.3175
5	FedFTG	0.7274
	FlexLoRA	0.6116
	FFA-LoRA	0.1104

Table 2: Comparison of F1 score on Brain Tumour Classification Dataset for fine-tuning SigLIP using different FL fine-tuning methods across non-IID splits

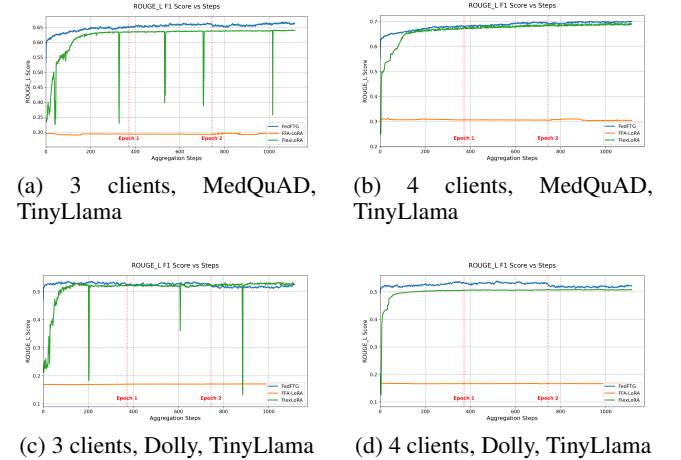


Figure 4: Variation of ROUGE_L scores evaluated on the test set with global aggregation steps across different clients and datasets for the TinyLlama model.

transformer models in federated environments that leverages GaLore’s efficient subspace learning mechanism. This framework demonstrates robust performance across vision and language transformer architectures, effectively addressing LoRA’s sub-optimal subspace learning bottlenecks while consistently outperforming existing approaches across diverse datasets and client configurations. By incorporating GaLore’s insights, we show how gradient subspace methods operating on parameter matrices can mitigate common federated learning bottlenecks, particularly preventing rank inflation and its associated excess risk increase. This success suggests that exploiting slowly evolving gradient subspaces could lead to more robust aggregation algorithms. Future research directions include developing more stable, parameter-efficient federated fine-tuning methods and exploring adaptive aggregation strategies for heterogeneous environments. Our work aims to guide the research community toward low-rank gradient-based optimization strategies, while the theoretical foundations established here could inform improved aggregation frameworks focusing on structured localized subspaces.

References

Abadi, M.; Chu, A.; Goodfellow, I.; McMahan, H. B.; Mironov, I.; Talwar, K.; and Zhang, L. 2016. Deep Learning with Differential Privacy. In *Proceedings of the 2016 ACM SIGSAC Conference on Computer and Communications Security*, CCS’16. ACM.

Alam, S.; Liu, L.; Yan, M.; and Zhang, M. 2022. FedRolex: Model-Heterogeneous Federated Learning with Rolling Sub-Model Extraction. In *NeurIPS*.

Ansell, A.; Ponti, E. M.; Korhonen, A.; and Vulic, I. 2022. Composable Sparse Fine-Tuning for Cross-Lingual Transfer. In *ACL (1)*, 1778 – 1796.

Babakniya, S.; Elkordy, A.; Ezzeldin, Y.; Liu, Q.; Song, K.-B.; EL-Khamy, M.; and Avestimehr, S. 2023. SLoRA: Federated Parameter Efficient Fine-Tuning of Language Models. In *International Workshop on Federated Learning in the Age of Foundation Models in Conjunction with NeurIPS 2023*.

Bai, J.; Chen, D.; Qian, B.; Yao, L.; and Li, Y. 2024. Federated Fine-tuning of Large Language Models under Heterogeneous Tasks and Client Resources. arXiv:2402.11505.

Ben Abacha, A.; and Demner-Fushman, D. 2019. A Question-Entailment Approach to Question Answering. *BMC Bioinform.*, 20(1): 511:1–511:23.

Brown, T. B.; Mann, B.; Ryder, N.; Subbiah, M.; Kaplan, J.; Dhariwal, P.; Neelakantan, A.; Shyam, P.; Sastry, G.; Askell, A.; Agarwal, S.; Herbert-Voss, A.; Krueger, G.; Henighan, T.; Child, R.; Ramesh, A.; Ziegler, D. M.; Wu, J.; Winter, C.; Hesse, C.; Chen, M.; Sigler, E.; Litwin, M.; Gray, S.; Chess, B.; Clark, J.; Berner, C.; McCandlish, S.; Radford, A.; Sutskever, I.; and Amodei, D. 2020. Language Models are Few-Shot Learners. In *NeurIPS*.

Cheng, J. 2017. brain tumor dataset.

Cho, Y. J.; Liu, L.; Xu, Z.; Fahrezi, A.; Barnes, M.; and Joshi, G. 2023. Heterogeneous LoRA for Federated Fine-tuning of On-device Foundation Models. In *International Workshop on Federated Learning in the Age of Foundation Models in Conjunction with NeurIPS 2023*.

Conover, M.; Hayes, M.; Mathur, A.; Xie, J.; Wan, J.; Shah, S.; Ghodsi, A.; Wendell, P.; Zaharia, M.; and Xin, R. 2023. Free Dolly: Introducing the World’s First Truly Open Instruction-Tuned LLM.

Diao, E.; Ding, J.; and Tarokh, V. 2021. HeteroFL: Computation and Communication Efficient Federated Learning for Heterogeneous Clients. In *ICLR*.

Ding, N.; Qin, Y.; Yang, G.; Wei, F.; Yang, Z.; Su, Y.; Hu, S.; Chen, Y.; Chan, C.-M.; Chen, W.; Yi, J.; Zhao, W.; Wang, X.; Liu, Z.; Zheng, H.-T.; Chen, J.; Liu, Y.; Tang, J.; Li, J.; and Sun, M. 2023. Parameter-efficient fine-tuning of large-scale pre-trained language models. *Nature Machine Intelligence*, 5(3): 220–235.

Dosovitskiy, A.; Beyer, L.; Kolesnikov, A.; Weissenborn, D.; Zhai, X.; Unterthiner, T.; Dehghani, M.; Minderer, M.; Heigold, G.; Gelly, S.; Uszkoreit, J.; and Houlsby, N. 2021. An Image is Worth 16x16 Words: Transformers for Image Recognition at Scale. In *International Conference on Learning Representations*.

Du, X.; Liu, M.; Wang, K.; Wang, H.; Liu, J.; Chen, Y.; Feng, J.; Sha, C.; Peng, X.; and Lou, Y. 2024. Evaluating Large Language Models in Class-Level Code Generation. In *Proceedings of the IEEE/ACM 46th International Conference on Software Engineering*, ICSE ’24. New York, NY, USA: Association for Computing Machinery. ISBN 9798400702174.

He, R.; Liu, L.; Ye, H.; Tan, Q.; Ding, B.; Cheng, L.; Low, J.-W.; Bing, L.; and Si, L. 2021. On the Effectiveness of Adapter-based Tuning for Pretrained Language Model Adaptation. In *ACL/IJCNLP (1)*, 2208 – 2222.

Houlsby, N.; Giurgiu, A.; Jastrzebski, S.; Morrone, B.; Laroussilhe, Q. d.; Gesmundo, A.; Attariyan, M.; and Gelly, S. 2019. Parameter-Efficient Transfer Learning for NLP. In *ICML*, 2790 – 2799.

Hsu, T.-M. H.; Qi, H.; and Brown, M. 2019. Measuring the Effects of Non-Identical Data Distribution for Federated Visual Classification. arXiv:1909.06335.

Hu, E. J.; Shen, Y.; Wallis, P.; Allen-Zhu, Z.; Li, Y.; Wang, S.; Wang, L.; and Chen, W. 2022. LoRA: Low-Rank Adaptation of Large Language Models. In *ICLR*.

Karimireddy, S. P.; Kale, S.; Mohri, M.; Reddi, S.; Stich, S.; and Suresh, A. T. 2020. SCAFFOLD: Stochastic Controlled Averaging for Federated Learning. In III, H. D.; and Singh, A., eds., *Proceedings of the 37th International Conference on Machine Learning*, volume 119 of *Proceedings of Machine Learning Research*, 5132–5143. PMLR.

Kirillov, A.; Mintun, E.; Ravi, N.; Mao, H.; Rolland, C.; Gustafson, L.; Xiao, T.; Whitehead, S.; Berg, A.; Lo, W.-Y.; Dollár, P.; and Girshick, R. B. 2023. Segment Anything. In *IEEE International Conference on Computer Vision*, 3992 – 4003.

Kuang, W.; Qian, B.; Li, Z.; Chen, D.; Gao, D.; Pan, X.; Xie, Y.; Li, Y.; Ding, B.; and Zhou, J. 2023. FederatedScope-LLM: A Comprehensive Package for Fine-tuning Large Language Models in Federated Learning. arXiv:2309.00363.

Lester, B.; Al-Rfou, R.; and Constant, N. 2021. The Power of Scale for Parameter-Efficient Prompt Tuning. In *EMNLP (1)*, 3045 – 3059.

Li, X. L.; and Liang, P. 2021. Prefix-Tuning: Optimizing Continuous Prompts for Generation. In *ACL/IJCNLP (1)*, 4582 – 4597.

Lin, C.-Y. 2004. ROUGE: A Package for Automatic Evaluation of Summaries. In *Text Summarization Branches Out*, 74–81. Barcelona, Spain: Association for Computational Linguistics.

Liu, H.; Li, C.; Wu, Q.; and Lee, Y. J. 2023. Visual Instruction Tuning. In *Thirty-seventh Conference on Neural Information Processing Systems*.

Loshchilov, I.; and Hutter, F. 2019. Decoupled Weight Decay Regularization. In *ICLR (Poster)*.

Mahla, N.; D’souza, A.; Gupta, S.; Kanekar, B.; and Jadhav, K. S. 2024. MedSAGA: Few-shot Memory Efficient Medical Image Segmentation using Gradient Low-Rank Projection in SAM. arXiv:2407.15042.

McMahan, B.; Moore, E.; Ramage, D.; Hampson, S.; and Arcas, B. A. y. 2017. Communication-Efficient Learning of Deep Networks from Decentralized Data. In Singh, A.; and Zhu, J., eds., *Proceedings of the 20th International Conference on Artificial Intelligence and Statistics*, volume 54 of *Proceedings of Machine Learning Research*, 1273–1282. PMLR.

Niu, Y.; Prakash, S.; Kundu, S.; Lee, S.; and Avestimehr, S. 2022. Federated Learning of Large Models at the Edge via Principal Sub-Model Training. In *Workshop on Federated Learning: Recent Advances and New Challenges (in Conjunction with NeurIPS 2022)*.

OpenAI. 2023. GPT-4 technical report. *arXiv*, 2303–08774.

Papineni, K.; Roukos, S.; Ward, T.; and Zhu, W.-J. 2002. Bleu: a Method for Automatic Evaluation of Machine Translation. In Isabelle, P.; Charniak, E.; and Lin, D., eds., *Proceedings of the 40th Annual Meeting of the Association for Computational Linguistics*, 311–318. Philadelphia, Pennsylvania, USA: Association for Computational Linguistics.

Qin, Z.; Chen, D.; Qian, B.; Ding, B.; Li, Y.; and Deng, S. 2024. Federated Full-Parameter Tuning of Billion-Sized Language Models with Communication Cost under 18 Kilobytes. *arXiv:2312.06353*.

Radford, A.; Kim, J. W.; Hallacy, C.; Ramesh, A.; Goh, G.; Agarwal, S.; Sastry, G.; Askell, A.; Mishkin, P.; Clark, J.; Krueger, G.; and Sutskever, I. 2021a. Learning Transferable Visual Models From Natural Language Supervision. In Meila, M.; and Zhang, T., eds., *Proceedings of the 38th International Conference on Machine Learning*, volume 139 of *Proceedings of Machine Learning Research*, 8748–8763. PMLR.

Radford, A.; Kim, J. W.; Hallacy, C.; Ramesh, A.; Goh, G.; Agarwal, S.; Sastry, G.; Askell, A.; Mishkin, P.; Clark, J.; et al. 2021b. Learning transferable visual models from natural language supervision. In *International conference on machine learning*, 8748–8763. PMLR.

Ruder, S. 2017. An overview of gradient descent optimization algorithms. *arXiv:1609.04747*.

Sun, J.; Mei, C.; Wei, L.; Zheng, K.; Liu, N.; Cui, M.; and Li, T. 2024a. Dial-insight: Fine-tuning Large Language Models with High-Quality Domain-Specific Data Preventing Capability Collapse. *ArXiv*, abs/2403.09167.

Sun, Y.; Li, Z.; Li, Y.; and Ding, B. 2024b. Improving LoRA in Privacy-preserving Federated Learning. In *The Twelfth International Conference on Learning Representations*.

Team, G.; Mesnard, T.; Hardin, C.; Dadashi, R.; Bhupatiraju, S.; Pathak, S.; Sifre, L.; Rivière, M.; Kale, M. S.; Love, J.; Tafti, P.; Hussenot, L.; Sessa, P. G.; Chowdhery, A.; Roberts, A.; Barua, A.; Botev, A.; Castro-Ros, A.; Slone, A.; Héliou, A.; Tacchetti, A.; Bulanova, A.; Patterson, A.; Tsai, B.; Shahriari, B.; Lan, C. L.; Choquette-Choo, C. A.; Crepy, C.; Cer, D.; Ippolito, D.; Reid, D.; Buchatskaya, E.; Ni, E.; Noland, E.; Yan, G.; Tucker, G.; Muraru, G.-C.; Rozhdestvenskiy, G.; Michalewski, H.; Tenney, I.; Grishchenko, I.; Austin, J.; Keeling, J.; Labanowski, J.; Lespiau, J.-B.; Stanway, J.; Brennan, J.; Chen, J.; Ferret, J.; Chiu, J.; Mao-Jones, J.; Lee, K.; Yu, K.; Millican, K.; Sjoesund, L. L.; Lee, L.; Dixon, L.; Reid, M.; Mikuła, M.; Wirth, M.; Sharman, M.; Chinaev, N.; Thain, N.; Bachem, O.; Chang, O.; Wahltinez, O.; Bailey, P.; Michel, P.; Yotov, P.; Chaabouni, R.; Comanescu, R.; Jana, R.; Anil, R.; McIlroy, R.; Liu, R.; Mullins, R.; Smith, S. L.; Borgeaud, S.; Girgin, S.; Douglas, S.; Pandya, S.; Shakeri, S.; De, S.; Klimenko, T.; Hennigan, T.; Feinberg, V.; Stokowiec, W.; hui Chen, Y.; Ahmed, Z.; Gong, Z.; Warkentin, T.; Peran, L.; Giang, M.; Farabet, C.; Vinyals, O.; Dean, J.; Kavukcuoglu, K.; Hassabis, D.; Ghahramani, Z.; Eck, D.; Barral, J.; Pereira, F.; Collins, E.; Joulin, A.; Fiedel, N.; Senter, E.; Andreev, A.; and Kenealy, K. 2024. Gemma: Open Models Based on Gemini Research and Technology. *arXiv:2403.08295*.

Tian, Y.; Wang, Y.; Zhang, Z.; Chen, B.; and Du, S. S. 2024. JoMA: Demystifying Multilayer Transformers via Joint Dynamics of MLP and Attention. In *The Twelfth International Conference on Learning Representations*.

Touvron, H.; Lavril, T.; Izacard, G.; Martinet, X.; Lachaux, M.-A.; Lacroix, T.; Rozière, B.; Goyal, N.; Hambro, E.; Azhar, F.; et al. 2023. Llama: Open and efficient foundation language models. *arXiv preprint arXiv:2302.13971*.

Vaswani, A.; Shazeer, N.; Parmar, N.; Uszkoreit, J.; Jones, L.; Gomez, A. N.; Kaiser, L.; and Polosukhin, I. 2017. Attention is All you Need. In *NIPS*, 5998 – 6008.

Woisetschläger, H.; Erben, A.; Marino, B.; Wang, S.; Lane, N. D.; Mayer, R.; and Jacobsen, H.-A. 2024. Federated Learning Priorities Under the European Union Artificial Intelligence Act. *arXiv:2402.05968*.

Xu, A.; and Raginsky, M. 2017. Information-theoretic analysis of generalization capability of learning algorithms. *Advances in neural information processing systems*, 30.

Zeng, A.; Liu, X.; Du, Z.; Wang, Z.; Lai, H.; Ding, M.; Yang, Z.; Xu, Y.; Zheng, W.; Xia, X.; et al. 2022. GLM-130B: An Open Bilingual Pre-trained Model. In *The Eleventh International Conference on Learning Representations*.

Zhai, X.; Mustafa, B.; Kolesnikov, A.; and Beyer, L. 2023. Sigmoid Loss for Language Image Pre-Training. In *ICCV*, 11941 – 11952.

Zhang, J.; Vahidian, S.; Kuo, M.; Li, C.; Zhang, R.; Yu, T.; Wang, G.; and Chen, Y. 2024a. Towards Building The Federatedgpt: Federated Instruction Tuning. In *ICASSP 2024 - 2024 IEEE International Conference on Acoustics, Speech and Signal Processing (ICASSP)*.

Zhang, P.; Zeng, G.; Wang, T.; and Lu, W. 2024b. TinyLlama: An Open-Source Small Language Model. *arXiv:2401.02385*.

Zhang, S.; Roller, S.; Goyal, N.; Artetxe, M.; Chen, M.; Chen, S.; Dewan, C.; Diab, M.; Li, X.; Lin, X. V.; et al. 2022. Opt: Open pre-trained transformer language models. *arXiv preprint arXiv:2205.01068*.

Zhao, J.; Zhang, Z.; Chen, B.; Wang, Z.; Anandkumar, A.; and Tian, Y. 2024. GaLore: Memory-Efficient LLM Training by Gradient Low-Rank Projection. In *Forty-first International Conference on Machine Learning*.

Zhu, J.; Greenewald, K.; Nadjahi, K.; Sáez De Ocáriz Borde, H.; Gabrielsson, R. B.; Choshen, L.; Ghassemi, M.;

Yurochkin, M.; and Solomon, J. 2024. Asymmetry in Low-Rank Adapters of Foundation Models. In Salakhutdinov, R.; Kolter, Z.; Heller, K.; Weller, A.; Oliver, N.; Scarlett, J.; and Berkenkamp, F., eds., *Proceedings of the 41st International Conference on Machine Learning*, volume 235 of *Proceedings of Machine Learning Research*, 62369–62385. PMLR.

Reproducibility Checklist

All the details related to the reproducibility checklist can be found in the supplementary material.

Proofs and Analysis

In this section, we present the proofs of proposition and theorems from the main paper and provide further analysis.

Proposition 1 *In FL scenarios like FlexLoRA, where parameter change matrices $\Delta \mathbf{W}_i$ from N clients are aggregated with each client i having an intrinsic rank r_i , the globally aggregated parameter matrix exhibits rank inflation following each global aggregation step. Specifically, in a scenario where all clients have identical ranks $r_i = r$ for simplicity, the rate of rank inflation, denoted by η satisfies $1 \leq \eta \leq N$ per global aggregation step.*

Proof:

Let the rank of the adapter matrix $\Delta \mathbf{W}_i$ from each client i be $\text{rank}(\Delta \mathbf{W}_i) = r_i$. For an aggregation scheme like FedAvg in FlexLoRA:

$$\Delta \mathbf{W}_{agg} = \frac{1}{N} \sum_{i=1}^N \Delta \mathbf{W}_i \quad (9)$$

For the summation of two low-rank matrices \mathbf{P} and \mathbf{Q} , the following bounds on the rank of the sum of the matrices are true:

$$\max(\text{rank}(\mathbf{P}), \text{rank}(\mathbf{Q})) \leq \text{rank}(\mathbf{P} + \mathbf{Q}) \leq \text{rank}(\mathbf{P}) + \text{rank}(\mathbf{Q}) \quad (10)$$

From equation (1) and (2), we can write:

$$\begin{aligned} \max(\text{rank}(\Delta \mathbf{W}_1), \text{rank}(\Delta \mathbf{W}_2), \dots, \text{rank}(\Delta \mathbf{W}_N)) &\leq \text{rank}\left(\sum_{i=1}^N \Delta \mathbf{W}_i\right) \leq \sum_{i=1}^N \text{rank}(\Delta \mathbf{W}_i) \\ \max(\text{rank}(\Delta \mathbf{W}_1), \text{rank}(\Delta \mathbf{W}_2), \dots, \text{rank}(\Delta \mathbf{W}_N)) &\leq \text{rank}\left(\sum_{i=1}^N \Delta \mathbf{W}_i\right) \leq \sum_{i=1}^N \text{rank}(\Delta \mathbf{W}_i) \end{aligned} \quad (11)$$

Since, multiplying by a scalar doesn't alter the rank of the matrix:

$$\max(\text{rank}(\Delta \mathbf{W}_1), \text{rank}(\Delta \mathbf{W}_2), \dots, \text{rank}(\Delta \mathbf{W}_N)) \leq \text{rank}(\Delta \mathbf{W}_{agg}) \leq \sum_{i=1}^N \text{rank}(\Delta \mathbf{W}_i) \quad (12)$$

This implies that the rank of the aggregated matrix will be at least greater than the maximum rank among all client LoRA adapter matrices, and at most equal to the sum of the individual ranks. Consequently, it can be inferred that the rank of the aggregated matrix will increase compared to the previous ranks. In the simplified scenario where $r_i = r$, the following conclusions can be drawn:

$$r \leq \text{rank}(\Delta \mathbf{W}_{agg}) \leq Nr \quad (13)$$

As a result, the rank can increase by a factor ranging from 1 to N . The rank of the aggregated matrix will stay the same in the case when the individual client LoRA adapter matrices $\Delta \mathbf{W}_i$ lie in the same subspace, which isn't possible in the case when there are non-IID datasets present which can differ the subspaces across the clients.

Proposition 1 highlights the constrained subspaces within FlexLoRA. In FlexLoRA, even though the rank is inflated after aggregation, the low-rank decomposition is still performed based on the original, smaller rank r . This restriction hinders the subspace learning process, as it involves decomposing the aggregated matrix into low-rank matrices with ranks smaller than the intrinsic rank of the original aggregated matrix. This limitation can impede the model's ability to fully capture the underlying data distribution across clients.

Lemma 1 *In FFA-LoRA, the total weight update of the complete LoRA adapter matrix $\Delta \mathbf{W}$ can be written in terms of the gradient of that at each iteration step with a learning rate α . At the end of T iterations, the following holds:*

$$\Delta \mathbf{W} = -\alpha \sum_{t=0}^T \nabla_{\mathbf{W}} \mathcal{L}_t(\mathbf{A}_0^\top \mathbf{A}_0) \quad (14)$$

The complete LoRA adapter matrix after weight aggregation (FedAvg) is equivalent to FedAvg aggregation of gradients at each local training iteration.

$$\Delta \mathbf{W}_{agg} = -\frac{\alpha}{N} \sum_{i=1}^N \sum_{t=0}^T \nabla_{\mathbf{W}} \mathcal{L}_t^{(i)}(\mathbf{A}_0^\top \mathbf{A}_0) = -\alpha \sum_{t=0}^T \left\{ \frac{1}{N} \sum_{i=1}^N \nabla_{\mathbf{W}} \mathcal{L}_t^{(i)} \right\} (\mathbf{A}_0^\top \mathbf{A}_0) \quad (15)$$

Proof:

For updating a pre-trained weight matrix $\mathbf{W}_0 \in \mathbb{R}^{d \times k}$, LoRA parameters $\mathbf{B} \in \mathbb{R}^{d \times r}$ and $\mathbf{A} \in \mathbb{R}^{r \times k}$ with $r \ll \min(d, k)$, forward pass in LoRA can be written as:

$$\mathbf{y} = (\mathbf{W}_0 + \mathbf{B} \mathbf{A}) \mathbf{x} \quad (16)$$

where $\mathbf{x} \in \mathbb{R}^k$ is the input to the current layer and $\mathbf{y} \in \mathbb{R}^d$ is the output which is passed to the next layer. During backpropagation:

$$\nabla_{\mathbf{W}} \mathcal{L} = \nabla_{\mathbf{y}} \mathcal{L} \mathbf{x}^{\top} \quad (17)$$

Since we fine-tune either parameter \mathbf{B} or \mathbf{A} , we need to express the gradient with respect to these parameters in terms of the gradient of the pre-trained matrix. In FFA-LoRA, where we exclusively fine-tune the zero-initialized LoRA parameters, the gradient can be expressed as follows:

$$\nabla_{\mathbf{B}} \mathcal{L} = \nabla_{\mathbf{W}} \mathcal{L} \mathbf{A}_0^{\top} \quad (18)$$

The update of the zero-initialized LoRA parameter can be written as:

$$\mathbf{B} := \mathbf{B} - \alpha \nabla_{\mathbf{B}} \mathcal{L}$$

where α is the learning rate. For updated value after T iterations can be written as:

$$\mathbf{B}_T = -\alpha \sum_{t=0}^T \nabla_{\mathbf{B}} \mathcal{L}_t \quad (19)$$

The following can be written for an update of the complete LoRA adapter matrix:

$$\Delta \mathbf{W} = -\alpha \sum_{t=0}^T \nabla_{\mathbf{B}} \mathcal{L}_t \mathbf{A}_0$$

From equation (11):

$$\Delta \mathbf{W} = -\alpha \sum_{t=0}^T \nabla_{\mathbf{B}} \mathcal{L}_t \mathbf{A}_0 = -\alpha \sum_{t=0}^T (\nabla_{\mathbf{W}} \mathcal{L}_t) \mathbf{A}_0^{\top} \mathbf{A}_0 \quad (20)$$

Post global aggregation (FedAvg), the weight changes will be averaged and thus giving us our equation (7).

Theorem 1 For a convex loss \mathcal{L} , let $\Delta \mathbf{W}^* \in \mathbb{R}^{d \times k}$ ($r \ll \min(d, k)$) be the optimal LoRA parameter matrix, α be the learning rate, and let the L2 norm of the gradient to be bounded (i.e. $\|\nabla_{\mathbf{W}} \mathcal{L}^{(i)}(\Delta \mathbf{W})\|_2 \leq D$). The excess risk ($|\mathcal{L}(\Delta \mathbf{W}_{agg}) - \mathcal{L}(\Delta \mathbf{W}^*)|$) bounds for the FFA-LoRA framework, involving N clients and S global aggregation steps having occurred every t_{agg} local training iterations, can be expressed as follows:

$$\leq D N S t_{agg} \left(D N S t_{agg} c + \frac{\alpha}{N} \|\Delta \mathbf{W}^*\|_2 \right) \quad (21)$$

Proof:

Let $\mathcal{L}(\Delta \mathbf{W})$ be the output loss of the model for the LoRA parameter $\Delta \mathbf{W}$. Let $\Delta \mathbf{W}^*$ be the most optimal LoRA adapter parameters. Assuming that the loss function $\mathcal{L}(\cdot)$ is convex, the excess risk can be written as:

$$\mathcal{L}(\Delta \mathbf{W}) - \mathcal{L}(\Delta \mathbf{W}^*) \leq \nabla_{\mathbf{W}} \mathcal{L}(\Delta \mathbf{W})^{\top} (\Delta \mathbf{W} - \Delta \mathbf{W}^*) \quad (22)$$

For the excess risk just after the aggregation, we can replace the weight parameters with the average of it.

$$\mathcal{L}(\Delta \mathbf{W}_{agg}) - \mathcal{L}(\Delta \mathbf{W}^*) \leq \nabla_{\mathbf{W}} \mathcal{L}(\Delta \mathbf{W}_{agg})^{\top} (\Delta \mathbf{W}_{agg} - \Delta \mathbf{W}^*) \quad (23)$$

$$\begin{aligned} |\mathcal{L}(\Delta \mathbf{W}_{agg}) - \mathcal{L}(\Delta \mathbf{W}^*)| &\leq \|\nabla_{\mathbf{W}} \mathcal{L}(\Delta \mathbf{W}_{agg})^{\top} (\Delta \mathbf{W}_{agg} - \Delta \mathbf{W}^*)\|_2 \\ &\leq \|\nabla_{\mathbf{W}} \mathcal{L}(\Delta \mathbf{W}_{agg})^{\top}\|_2 \|(\Delta \mathbf{W}_{agg} - \Delta \mathbf{W}^*)\|_2 \end{aligned} \quad (24)$$

Say a total of S global aggregation steps have happened, the LoRA adapter matrix can be written as:

$$\Delta \mathbf{W}_{S, t_{agg}} = \frac{-\alpha}{N} \sum_{i=1}^N \sum_{t=0}^{t_{agg}} \sum_{j=1}^S \nabla_{\mathbf{W}} \mathcal{L}_{t,j}^{(i)} (\mathbf{A}_0^{\top} \mathbf{A}_0) \quad (25)$$

Equation (16) can be further upper bounded by the summation of gradients at each iteration for S rounds of global aggregation (since the gradient just after the global aggregation can be written as an average of all the gradients at each time step for each client, see equation (7)):

$$\|\nabla_{\mathbf{W}} \mathcal{L}(\Delta \mathbf{W}_{S, t_{agg}})^{\top}\|_2 \|\Delta \mathbf{W}_{S, t_{agg}} - \Delta \mathbf{W}^*\|_2 \leq \sum_{i=1}^N \sum_{t=0}^{t_{agg}} \sum_{j=1}^S \|\nabla_{\mathbf{W}} \mathcal{L}_{t,j}^{(i)}(\Delta \mathbf{W}_{S, t_{agg}})\|_2 \|\Delta \mathbf{W}_{S, t_{agg}} - \Delta \mathbf{W}^*\|_2 \quad (26)$$

Which from Weyl's inequality can be further bounded as:

$$\|\nabla_{\mathbf{W}} \mathcal{L}(\Delta \mathbf{W}_{S,agg})^\top\|_2 \|\Delta \mathbf{W}_{S,agg} - \Delta \mathbf{W}^*\|_2 \leq \left\| \sum_{i=1}^N \sum_{t=0}^{t_{agg}} \sum_{j=1}^S \nabla_{\mathbf{W}} \mathcal{L}_{t,j}^{(i)}(\Delta \mathbf{W}_{S,agg}) \right\|_2 (\|\Delta \mathbf{W}_{S,agg}\|_2 + \|\Delta \mathbf{W}^*\|_2) \quad (27)$$

Expanding these equations:

$$\begin{aligned} & \leq \left\| \sum_{i=1}^N \sum_{t=0}^{t_{agg}} \sum_{j=1}^S \nabla_{\mathbf{W}} \mathcal{L}_{t,j}^{(i)}(\Delta \mathbf{W}_{S,agg}) \right\|_2^2 \left\| (\mathbf{A}_0^\top \mathbf{A}_0) \right\|_2 + \left\| \frac{-\alpha}{N} \sum_{i=1}^N \sum_{t=0}^{t_{agg}} \sum_{j=1}^S \nabla_{\mathbf{W}} \mathcal{L}_{t,j}^{(i)}(\Delta \mathbf{W}_{S,agg}) \right\|_2 \|\Delta \mathbf{W}^*\|_2 \\ & \leq \left\{ \sum_{i=1}^N \sum_{t=0}^{t_{agg}} \sum_{j=1}^S \left\| \nabla_{\mathbf{W}} \mathcal{L}_{t,j}^{(i)}(\Delta \mathbf{W}_{S,agg}) \right\|_2 \right\}^2 \left\| (\mathbf{A}_0^\top \mathbf{A}_0) \right\|_2 + \left| \frac{-\alpha}{N} \right| \sum_{i=1}^N \sum_{t=0}^{t_{agg}} \sum_{j=1}^S \left\| \nabla_{\mathbf{W}} \mathcal{L}_{t,j}^{(i)}(\Delta \mathbf{W}_{S,agg}) \right\|_2 \|\Delta \mathbf{W}^*\|_2 \end{aligned} \quad (28)$$

Let the term $\left\| \mathbf{A}_0^\top \mathbf{A}_0 \right\|_2$ be replaced by some constant c . Since the gradients are also assumed to be bounded, the entire equation (20) can be rewritten as:

$$|\mathcal{L}(\Delta \mathbf{W}_{agg}) - \mathcal{L}(\Delta \mathbf{W}^*)| \leq DNS t_{agg} \left(DNS t_{agg} c + \frac{\alpha}{N} \|\Delta \mathbf{W}^*\|_2 \right) \quad (29)$$

As the value of S increases, i.e. the number of global aggregation steps increases, the bounds on the excess risk keep on increasing.

Lemma 1 For a bounded gradient (L2 norm of the gradients upper bounded by D) L2 norm of the weight matrix in the GaLore-based FedAvg aggregation framework (like FedFTG) is upper bounded linearly by the number of global aggregation steps S and the number of local training steps between two consecutive aggregation steps t_{agg} :

$$\|\mathbf{W}_{agg}\| \leq B + \eta S t_{agg} D = \mathcal{O}(S t_{agg}) \quad (30)$$

where η is the learning rate and B is a constant.

Proof: Weight update for a client i at some time t_{agg} just before aggregation can be written as:

$$\mathbf{W}_{t_{agg}}^{(i)} = \mathbf{W}_0 - \eta \sum_{t=0}^{t_{agg}} \mathbf{G}_t^{(i)} \quad (31)$$

Now averaging the weights for FedAvg aggregation:

$$\mathbf{W}_{agg} = \mathbf{W}_0 - \frac{\eta}{N} \sum_{i=1}^N \sum_{t=0}^{t_{agg}} \mathbf{G}_t^{(i)}$$

Say, S rounds of communication have occurred, one can write the above equation as follows:

$$\mathbf{W}_{agg} = \mathbf{W}_0 - \frac{\eta}{N} \sum_{i=1}^N \sum_{j=0}^S \sum_{t=0}^{t_{agg}} \mathbf{G}_{t,j}^{(i)} \quad (32)$$

Taking L2 norm on both the sides:

$$\begin{aligned} \|\mathbf{W}_{agg}\| &= \left\| \mathbf{W}_0 - \frac{\eta}{N} \sum_{i=1}^N \sum_{j=0}^S \sum_{t=0}^{t_{agg}} \mathbf{G}_{t,j}^{(i)} \right\| \leq \|\mathbf{W}_0\| + \frac{\eta}{N} \sum_{i=1}^N \sum_{j=0}^S \sum_{t=0}^{t_{agg}} \|\mathbf{G}_{t,j}^{(i)}\| = \|\mathbf{W}_0\| + \frac{\eta}{N} \sum_{i=1}^N \sum_{j=0}^S \sum_{t=0}^{t_{agg}} D \\ &\implies \|\mathbf{W}_{agg}\| \leq B + \eta S t_{agg} D \end{aligned} \quad (33)$$

Assuming that L2 norm of initial weight matrix \mathbf{W}_0 is B and L2 norm of the gradient is bounded by D .

Theorem 2 For a convex loss function \mathcal{L} , let $\Delta \mathbf{W}^*$ denote the optimal weight matrix and α represent the learning rate. Assuming that the L2 norm of the gradient is bounded, specifically $\|\nabla_{\mathbf{W}} \mathcal{L}^{(i)}(\Delta \mathbf{W})\|_2 \leq D$, the excess risk, defined as $|\mathcal{L}(\Delta \mathbf{W}_{agg}) - \mathcal{L}(\Delta \mathbf{W}^*)|$, for the aggregated weights after a total of S direct FedAvg aggregations having occurred every t_{agg} local training iterations with GaLore as an optimizer can be expressed as follows:

$$|\mathcal{L}(\Delta \mathbf{W}_{agg}) - \mathcal{L}(\Delta \mathbf{W}^*)| \leq \alpha D^2 S t_{agg} + c = \mathcal{O}(S t_{agg}) \quad (34)$$

Here, c is a scalar constant.

Proof:

$$\mathcal{L}(\Delta \mathbf{W}) - \mathcal{L}(\Delta \mathbf{W}^*) \leq \nabla_{\mathbf{W}} \mathcal{L}(\Delta \mathbf{W})^\top (\Delta \mathbf{W} - \Delta \mathbf{W}^*) \quad (35)$$

For the excess risk just after the aggregation, we can replace the weight parameters with the average of it.

$$\mathcal{L}(\Delta \mathbf{W}_{agg}) - \mathcal{L}(\Delta \mathbf{W}^*) \leq \nabla_{\mathbf{W}} \mathcal{L}(\Delta \mathbf{W}_{agg})^\top (\Delta \mathbf{W}_{agg} - \Delta \mathbf{W}^*) \quad (36)$$

$$\begin{aligned} |\mathcal{L}(\Delta \mathbf{W}_{agg}) - \mathcal{L}(\Delta \mathbf{W}^*)| &\leq \|\nabla_{\mathbf{W}} \mathcal{L}(\Delta \mathbf{W}_{agg})^\top (\Delta \mathbf{W}_{agg} - \Delta \mathbf{W}^*)\|_2 \\ &\leq \|\nabla_{\mathbf{W}} \mathcal{L}(\Delta \mathbf{W}_{agg})^\top\|_2 \|(\Delta \mathbf{W}_{agg} - \Delta \mathbf{W}^*)\|_2 \end{aligned} \quad (37)$$

$$\begin{aligned} &\leq D(\alpha t_{agg} SD + k) \\ \implies |\mathcal{L}(\nabla \mathbf{W}_{agg}) - \mathcal{L}(\nabla \mathbf{W}^*)| &\leq \alpha D^2 S t_{agg} + c \end{aligned} \quad (38)$$

Theorem 3 Let N denote the number of clients, each possessing a dataset with n samples. We consider the weights of a lower-level MLP layer represented by $\mathbf{W} \in \mathbb{R}^{d \times k}$. Under the assumption that the risk function of each client is σ -sub-Gaussian with respect to the data distribution of that client and the corresponding weight matrix, we derive the following generalization error bounds for weight aggregation:

a) For federated fine-tuning using FFA-LoRA:

$$\mathcal{E}_1 \leq \frac{1}{N} \sum_{i=1}^N \sqrt{\frac{2\sigma^2 \ln 2}{n} r q \sum_i (d)} \quad (39)$$

b) or direct weight aggregation using FedAvg with a low-rank gradient-based optimizer, such as GaLore:

$$\mathcal{E}_2 \leq \frac{1}{N} \sum_{i=1}^N \sqrt{-\frac{2\sigma^2}{n} \sum_{j=1}^d \sum_{l=1}^k f(\mathbf{W}_i^{(j)}[l], t) \log \left(f(\mathbf{W}_i^{(j)}[l], t) \right)} \quad (40)$$

where $\mathbf{W}_i^{(j)}[l]$ represents the element of l th index in the j th row of the matrix \mathbf{W}_i . Here, $f(\mathbf{W}_i^{(j)}[l], t) = \frac{\exp(\mathbf{W}_i^{(j)}[l])}{\sum_{l=1}^k \exp(\mathbf{W}_i^{(j)}[l])}$ be the function to represent the ratio (probability) in a succinct manner. Also, as $t \rightarrow \infty$, i.e. as the federated training continues $f(\mathbf{W}_i^{(j)}[l], t) \rightarrow \frac{1}{k}$.

Proof:

Proof of this theorem follows from information-theoretic analysis. Generalization error is defined as the difference between the population and empirical risk. For N client system with non-i.i.d. dataset population risk can be defined as:

$$L_{\mu_1, \mu_2, \dots, \mu_N}(w) \triangleq \mathbb{E}_i[\mathbb{E}_Z[l_i(w, Z)]] = \mathbb{E}_i[\int_z l_i(w, z) \mu_i(dz)] \quad (41)$$

Where μ_i is the data distribution for client i and Z is a sample from the dataset.

Empirical risk can be written as:

$$L_{S_1, S_2, \dots, S_N}(w) \triangleq \mathbb{E}_i[\frac{1}{n} \sum_{j=1}^n l_j(w, Z_j)] \quad (42)$$

Where S_i is the dataset at client i . The total generalization error for a N client system can be written as:

$$|g(\mu_1, \mu_2, \dots, \mu_N; P_{W|S_1, S_2, \dots, S_N})| \leq \mathbb{E}_i[\mathbb{E}_Z[l_i(w, Z)]] - \mathbb{E}_i[\frac{1}{n} \sum_{j=1}^n l_j(w, Z_j)] \quad (43)$$

$$\implies |g(\mu_1, \mu_2, \dots, \mu_N; P_{W|S_1, S_2, \dots, S_N})| \leq \mathbb{E}_i[\mathbb{E}_Z[l_i(w, Z)] - \frac{1}{n} \sum_{j=1}^n l_j(w, Z_j)] = \frac{1}{N} \sum_{i=1}^N \left(\mathbb{E}_Z[l_i(w, Z)] - \frac{1}{n} \sum_{j=1}^n l_j(w, Z_j) \right)$$

The expression just inside the bracket is the generalization error for a single client system. As done the analysis thoroughly in the paper (Xu and Raginsky 2017), the generalization error for a single client system can be written as:

$$|g(\mu; P_{W|S})| \leq \sqrt{\frac{2\sigma^2}{n} I(S; W)} \quad (44)$$

From the paper (Zhu et al. 2024) which does the centralized training information-theoretic analysis of for LoRA based systems, including system closely resembling FFA-LoRA, we can directly replace the under-root term with the final expression from that paper:

$$|g(\mu_1, \mu_2, \dots, \mu_N; P_{W|S_1, S_2, \dots, S_N})| \leq \frac{1}{N} \sum_{i=1}^N \sqrt{\frac{2\sigma^2 \ln 2}{n} rq \sum_i (d)} \quad (45)$$

Continuing from equation 44 for case 9b), we can't directly write the entropy in the way similar to what we did in case (a). Lemma B.6 from the GaLore paper explains about the dynamics of weight matrix and gradient matrix rows while training. It shows that as the time proceeds, one of the row become extremely large than the others. In FL, when such matrices with infinitely large row values are aggregated together return a new matrix that has more number of rows with infinitely large row values. Since the values are infinitely large, they can be attributed to a near-similar value. We write the entropy for such a system as:

$$H = - \sum_{j=1}^d \sum_{l=1}^k p(\mathbf{W}_{(j,l)}) \log(p(\mathbf{W}_{(j,l)})) \quad (46)$$

The expression of probability can be replaced by the function f that can be described as: $f(\mathbf{W}_i^{(j)}[l], t) = \frac{\exp(\mathbf{W}_i^{(j)}[l])}{\sum_{l=1}^k \exp(\mathbf{W}_i^{(j)}[l])}$. Plugging in this expression in the expression of entropy which upper bounds mutual entropy in equation 44 gives us the expression from case (b).

For the expression of generalization error for FFA-LoRA (case (c)) can be directly derived by plugging in the value generalization to equation (49) from the analysis performed by (Zhu et al. 2024) (Lemma 4.5 of the paper) for the generalization error bound of using LoRA in centralized settings.

Datasets and Experiments

In this section, we discuss about the datasets and their pre-processing. We also discuss about the experiment setup in detail along with the hyperparameters used.

Dataset Preparation

We utilized the MedQuAD and Dolly-15k datasets as outlined in the main paper. The entire Dolly-15k dataset was employed for distributed training, while for MedQuAD, we sampled 15k instances proportionately from the main dataset. The MedQuAD dataset, as reported by its authors, originally contains 39 question types related to various medical topics such as diseases and drugs. However, due to MedlinePlus copyright restrictions, answers from three subsets were removed, resulting in approximately 31,034 void cells lacking answers. After excluding these void cells, we were left with 16,407 valid QnA pairs and 16 unique question types. From these, we proportionately sampled 15k pairs. For the Dolly-15k dataset, the entire dataset was used since it closely matched the target sample size of 15,000.

To prepare non-IID shards, we employed Dirichlet allocation to assign class label distributions to each shard/client. The shards were created to ensure an equal number of samples per shard. Dirichlet Allocation was used to determine the proportion of each class (*question_type* in MedQuAD and *instruction_category* in Dolly-15k) assigned to each client, with a concentration parameter of $\alpha = 0.1$. Smaller α values result in more skewed distributions, thus simulating more realistic non-IID scenarios. During the assignment of samples to each shard, no replacement was considered, meaning a sample assigned to one shard was not reassigned to another. The Brain Tumor Classification dataset was partitioned in a similar manner. MedQuAD and Dolly-15k were split into 4 shards, while the Brain Tumor Classification Dataset was divided into 5 shards. These shards were then allocated to participating clients, with client i assigned to shard i . The label distribution for each shard is shown in the main paper. Notably, each shard in Dolly-15k and MedQuAD contains approximately 3,714 and 3,712 samples, respectively.

The reason we choose these datasets is to diversify the type of downstream tasks and the type of dataset. Dolly-15k dataset is more generic and thus semantically more prevalent in the pre-training/instruction-tuning corpus of the LLMs unlike the MedQuAD dataset which showcases our method's efficiency on datasets which are out of distribution with the pre-training context of the LLM. Similar reason why we choose a medical dataset (Brain Tumor Classification Dataset) for our experiments. Since ViTs pre-training corpus already have the context of the generic images, we instead advocate the use for medical images like Brain MRI scans which may not be directly present during pre-training thus letting us conclude the performance of the ViT trained using different FL frameworks in the cases when the dataset to fine-tune is out of distribution with the pre-training corpus.

For evaluation, each shard was split into training and test sets, with the test set size comprising 1% of the total shard size. The test sets from different shards were combined to form a global evaluation set, resulting in a test set size equivalent to 37 times the number of clients N for both Dolly-15k and MedQuAD. A similar approach was applied to the Brain Tumor Classification dataset, with the difference being the test set size, which was set to 5% of the total shard size. Each shard of the Brain Tumor Classification Dataset contains approximately 582 samples, resulting in a global evaluation set of size $N \times 29$ samples, where N is the number of clients. This non-IID dataset splitting process was conducted twice, producing distinct label distributions

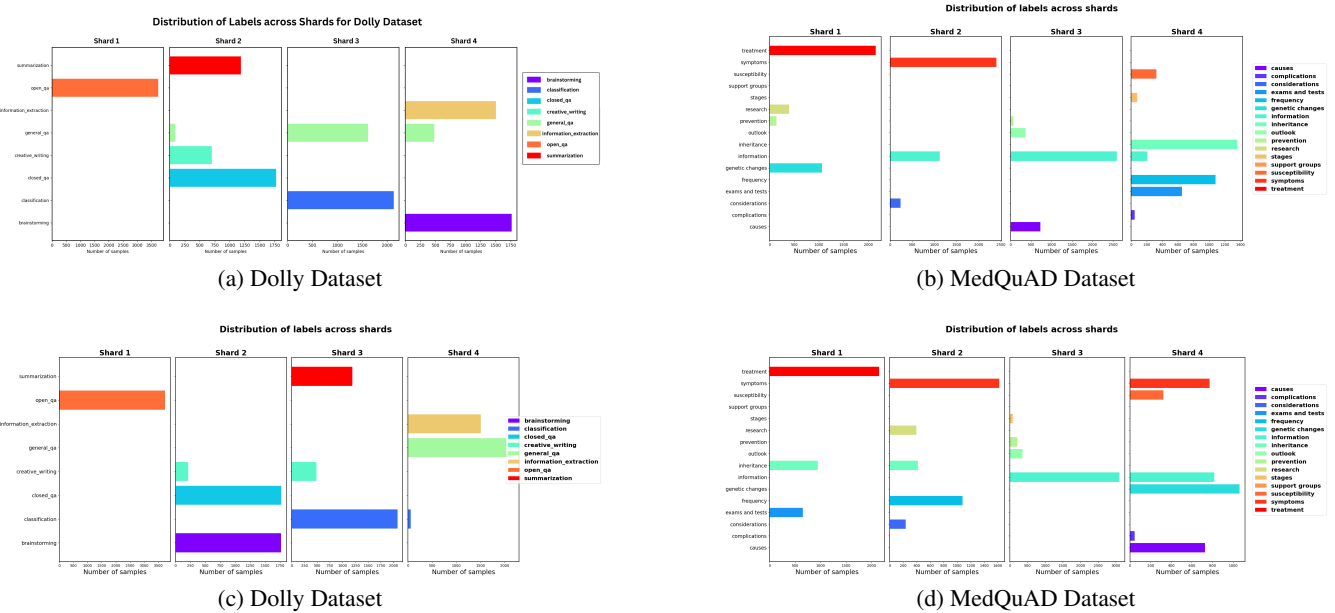


Figure 5: Label distribution across shards for Dolly and MedQuAD datasets produced using Dirichlet Allocation with $\alpha = 0.1$. Figure 1(a) and 1(b) show the label distributions which are used in the main paper, and fig. 1(c) and 1(d) are the new label distributions whose experimental results are shown in this supplementary material.

across shards. The results from one of these splits are presented in the main paper, while the experiments and results from the second split are discussed here.

Experiments

In this section, we provide a detailed overview of the experimental setup and present additional experimental results. As mentioned in the main paper, all experiments were conducted on a single Nvidia A6000 cluster. One of the GPUs in this cluster functioned as the server, handling global aggregation, while the remaining GPUs were utilized for hosting models to perform local training iterations on non-IID datasets.

For the FlexLoRA and FFA-LoRA experiments on text modality, we selected a LoRA rank of 8 and a scaling factor of 16, consistent with the hyperparameters used in the original papers for these methods. In the FedFTG experiments, the main results reported in the paper were obtained by fine-tuning the *project-up* MLP layer.

In the vision dataset experiments, we used a LoRA rank of 8 and a scaling factor of 32 for both FlexLoRA and FFA-LoRA, with a batch size of 2, in contrast to the batch size of 1 used for the text dataset experiments. For FedFTG, we fine-tuned both the classifier layer and the project-up layer, whereas in FlexLoRA and FFA-LoRA, only the attention parameters (Q, K, V) were fine-tuned. We applied GaLore to the final classifier layer of the transformer, as the Feed-Forward Network (FFN) layer in a neural network with a softmax objective can be represented in a parametric form that becomes low-rank during training (refer to Theorem 3.2 and Lemma 3.3 in the GaLore paper).

Figures 1(a) and 1(b) illustrate the label distributions for the Dolly-15k and MedQuAD datasets, representing the client label configurations used in the main paper's experiments. Figures 1(c) and 1(d) depict alternative label distributions, distinct from those in the main paper. The next section presents the experimental results corresponding to this alternate client label configuration. As far as computational overhead is concerned, FedFTG takes about 20GBs in contrast to 14.2GBs taken by LoRA methods (FlexLoRA and FFA-LoRA) on Nvidia RTX A6000 GPU. This can be attributed to the fact that FedFTG isn't as parameter-efficient as LoRA is. This is part of the future research to innovate on more parameter-efficient fine-tuning methods which do not use LoRA.

Analysis of the Experiments Performed in the Main Paper In this section, we provide a comprehensive discussion of the experiments conducted on the client label distributions presented in the main paper (Figures 1(a), 1(b), and 2(b)). The results in Table 1 of the main paper clearly indicate that FedFTG consistently outperforms both FFA-LoRA and FlexLoRA across multiple datasets, models, and numbers of clients.

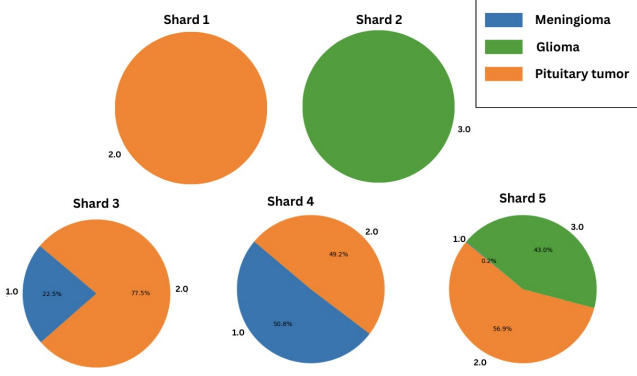
In the vision dataset experiments detailed in the main paper, FedFTG continues to outperform both LoRA-based federated learning methods. The notably poorer performance of FFA-LoRA across both text and vision modalities aligns with the theoretical analysis provided earlier. According to Theorem 1, excess risk bounds increase with each FedAvg step, causing FFA-LoRA

No of Clients	Dataset	Model	Method	BLEU-4 Score	ROUGE-L Score	
3	MedQuAD	TinyLlama	FedFTG	0.5697	0.73	
			FlexLoRA	0.4691	0.6527	
			FFA-LoRA	0.0995	0.2585	
		Gemma-2B	FedFTG	0.5418	0.69	
			FlexLoRA	0.417	0.6317	
	Dolly-15K	TinyLlama	FFA-LoRA	0.0987	0.2919	
			FedFTG	0.2954	0.5277	
			FlexLoRA	0.2928	0.5234	
		Gemma-2B	FFA-LoRA	0.0552	0.1576	
			FedFTG	0.3294	0.5433	
4	MedQuAD	TinyLlama	FlexLoRA	0.2721	0.5288	
			FFA-LoRA	0.0642	0.1568	
		Gemma-2B	FedFTG	0.5962	0.7198	
			FlexLoRA	0.495	0.6722	
		Dolly-15K	FFA-LoRA	0.1131	0.2901	
	Dolly-15K		FedFTG	0.585	0.7254	
			FlexLoRA	0.5313	0.6969	
			FFA-LoRA	0.1141	0.2736	
	TinyLlama	FedFTG	0.3597	0.5354		
		FlexLoRA	0.2922	0.5022		
		FFA-LoRA	0.0677	0.1707		
	Gemma-2B	FedFTG	0.3513	0.5556		
		FlexLoRA	0.2723	0.5131		
		FFA-LoRA	0.0604	0.1716		

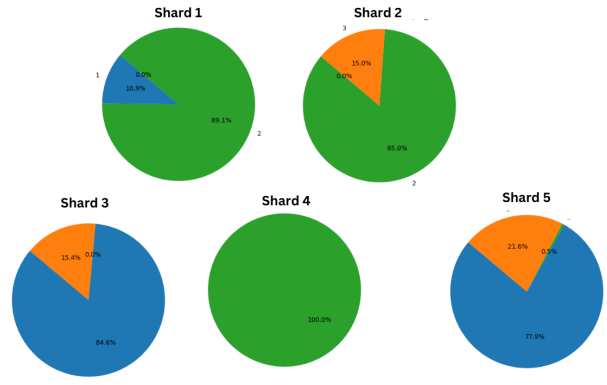
Table 3: Comparison of BLEU-4 and ROUGE L F1 scores across different methods, models, and datasets for varying client numbers with non-IID splits (see fig. 1(c) and 1(d))

No of clients	Method	F1 Score
3	FedFTG	0.7216
	FlexLoRA	0.5136
	FFA-LoRA	0.4533
4	FedFTG	0.7012
	FlexLoRA	0.6065
	FFA-LoRA	0.3639
5	FedFTG	0.8512
	FlexLoRA	0.4975
	FFA-LoRA	0.3894

Table 4: Comparison of F1 score on Brain Tumour Classification Dataset for fine-tuning SigLIP using different FL fine-tuning methods across non-IID splits (see fig. 2(b))



(a) Distribution of labels across shards for Brain Tumour Dataset produced using Dirichlet Allocation with $\alpha = 0.1$



(b) Second distribution of labels across shards for Brain Tumour Dataset produced using Dirichlet Allocation with $\alpha = 0.1$

Figure 6: Comparison of label distributions across different methods.

to deviate from the optimal parameters. This deviation results in inefficient learning of the dataset’s semantics across clients and, consequently, poorer performance. Figure 8 illustrates the variation of ROUGE_L F1 scores evaluated on the global evaluation set with the FedAvg aggregation steps for both the TinyLlama and Gemma-2B models. The figure highlights FFA-LoRA’s ineffective aggregation, as evidenced by its consistent underperformance and minimal improvements with increasing FedAvg steps.

In contrast, while FlexLoRA shows significant performance dips on the MedQuAD dataset, it still achieves reasonable aggregation efficiency but falls short compared to FedFTG. FedFTG demonstrates the most stable aggregation results, with minimal abrupt drops and consistent training performance. The graphs indicate that FedFTG maintains stable distributed training while outperforming both FlexLoRA and FFA-LoRA across various clients, datasets, and downstream tasks.

The vision modality experiments were carried out on dataset shards depicted in Figure 3. Table 2 shows that performance initially improves with 4 clients but declines with 5 clients. The main paper provides a detailed analysis of FedFTG and FFA-LoRA for the vision dataset. Here, we focus on the behavior of FlexLoRA in the vision dataset. FlexLoRA exhibits a different dynamic compared to FedFTG and FFA-LoRA due to its unique aggregation scheme. It tends to overfit when training with 4 clients, likely because the same labels are present in both shard 3 and shard 4. However, performance improves when expanding to 5 clients, as the model can potentially learn new representations from the additional data samples in the fifth shard, thereby enhancing its generalization capability.

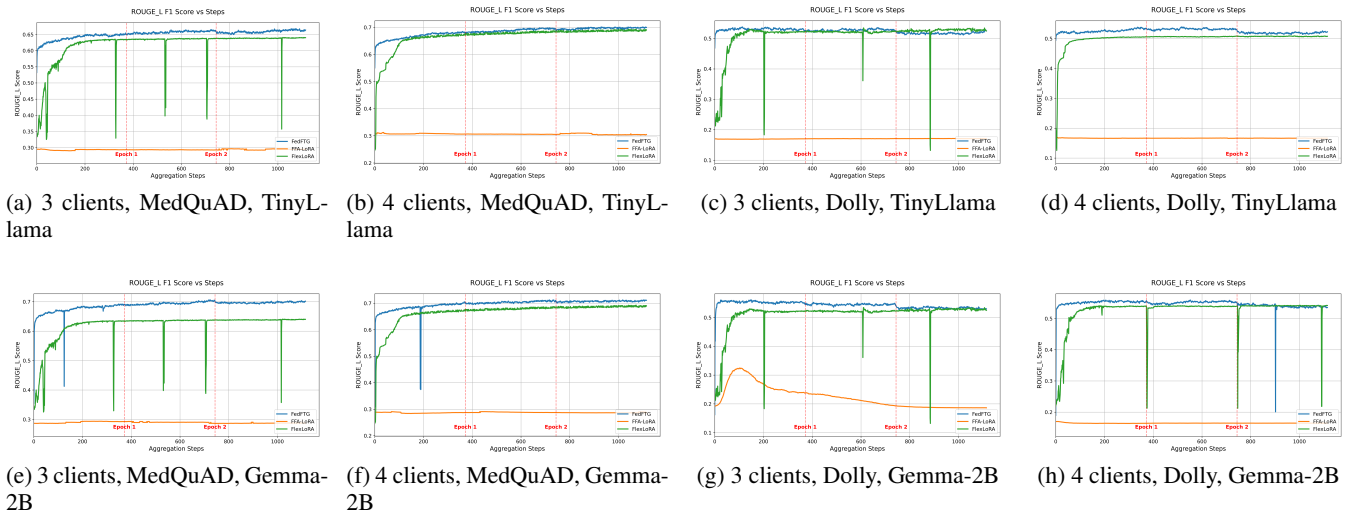


Figure 7: Variation of ROUGE_L scores evaluated on the test set with global aggregation steps across different clients and datasets for the TinyLlama model on the older label distributions (see Fig. 1(a) and 1(b))

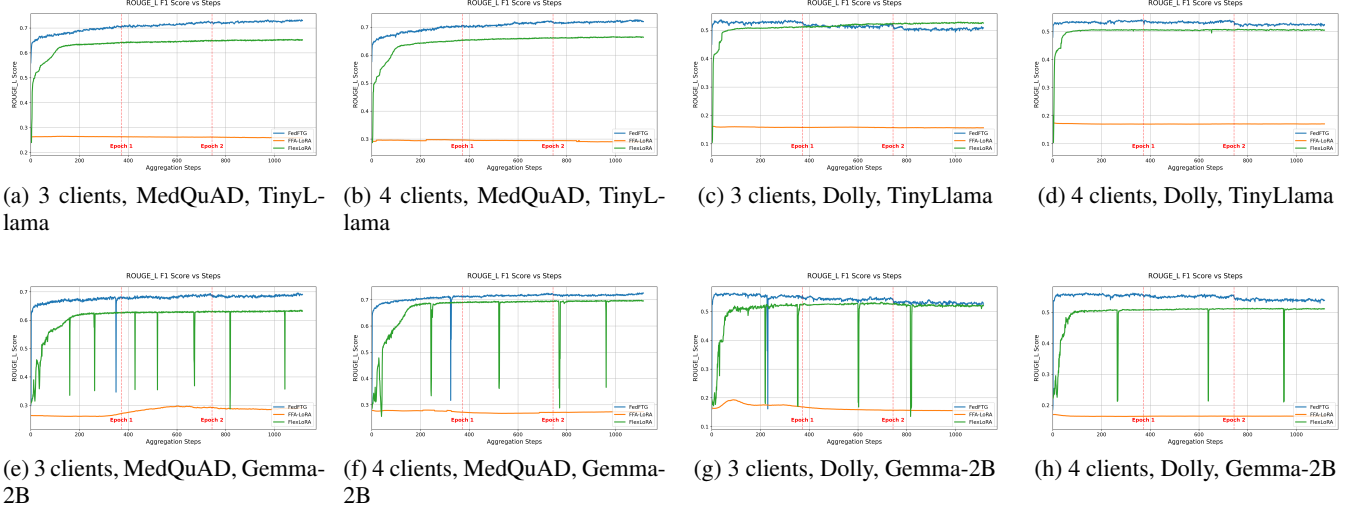


Figure 8: Variation of ROUGE_L scores evaluated on the test set with global aggregation steps across different clients and datasets for the TinyLlama model on the older label distributions (see Fig. 1(c) and 1(d))

Experiment Results on Different Label Distributions In this section, we perform our experiments on a label distribution which is different than the one used in the main paper. The new labels are shown in Fig 2(c), 2(d) (for text modality) and Fig 3(b) (for image modality).

As demonstrated in the table summarizing results on the new data distribution, FedFTG consistently outperforms both FlexLoRA and FFA-LoRA. Specifically, Table 1 shows that FedFTG surpasses these methods across both the MedQuAD and Dolly-15k datasets. Additionally, FedFTG outperforms other federated learning (FL) methods on SigLIP for the Brain Tumor Classification Dataset. Figure 4 further corroborates FedFTG’s superior performance, consistent with the findings from the main paper.

In line with the results observed for the label distributions in Figures 1(a) and 1(b) of the main paper, FedFTG tends to overfit on the Dolly-15k dataset for both 3 and 4 clients. Its performance graph is notably smoother, with minimal sudden dips, indicating stable aggregation and distributed learning. One potential reason for overfitting in the Dolly-15k dataset is that the context of Dolly-15k may already be present in the pre-training or instruction-tuning corpus of these large language models (LLMs). Given that Dolly-15k is a more generic dataset, LLMs are likely to have a prior understanding of its semantics, unlike the MedQuAD dataset, which is less prevalent in pre-training corpora.

As discussed in the main paper, accuracy is highly dependent on the interaction between labels, which results in variations in the metric values. In the new label distributions (see Fig. 6b), the accuracy of FedFTG and FFA-LoRA decreases as the number of clients increases. This decline is likely due to an underfitting scenario where the models trained using FedFTG and FFA-LoRA may not have adequately learned the semantics of shard 3, which contains labels 1 and 3, with label 3 only being present in shard 1 at a very small percentage. However, when the number of clients increases to 5, the performance of both FedFTG and FFA-LoRA improves. Notably, FedFTG performs even better with 5 clients than with 3 clients, while FFA-LoRA performs better than with 4 clients but still falls short of its performance with 3 clients. This highlights FedFTG’s superior generalization in this scenario, outperforming FFA-LoRA which is evident from our theoretical analysis as well.

Similar to the experiments discussed in the main paper, FlexLoRA exhibits a different behavior, with performance improving in the case of 4 clients but decreasing when the number of clients increases to 5.

All these experimental results show FedFTG’s superior performance over the current and the most recent State-of-the-Art (SOTA) FL methods which are based on LoRA. FedFTG is theoretically motivated and empirically verified across both image and text modalities on language and vision transformers. It effectively addresses LoRA’s bottlenecks related to sub-optimal sub-space learning and consistently outperforms FlexLoRA and FFA-LoRA across different datasets, multiple client configurations and experiment runs.

Reproducibility Checklist

In this section we answer the questions for reproducibility checklist as mentioned in the AAAI 2025 guidelines.

This paper:

- Q. Includes a conceptual outline and/or pseudocode description of AI methods introduced. Ans : **Yes**
- Q. Clearly delineates statements that are opinions, hypothesis, and speculation from objective facts and results. Ans: **Yes**
- Q. Provides well marked pedagogical references for less-familiar readers to gain background necessary to replicate the paper.

Ans: **Yes**

Does this paper make theoretical contributions? Ans: **Yes**

If yes, please complete the list below.

All assumptions and restrictions are stated clearly and formally. Ans: **Yes**

All novel claims are stated formally (e.g., in theorem statements). Ans: **Yes**

Proofs of all novel claims are included. Ans: **Yes, the proofs are all included in the supplementary material.**

Proof sketches or intuitions are given for complex and/or novel results. Ans: **Yes**

Appropriate citations to theoretical tools used are given. Ans: **Yes**

All theoretical claims are demonstrated empirically to hold. Ans: **Yes**, as discussed in the main paper as well as the supplementary material, the theoretical claims made for FlexLoRA (proposition 1) and FFA-LoRA (Theorem 1) hold true as their performance degradation aligns closely to how the model performs with different FL methods. Claims regarding FedFTG's stable aggregation and performance (Theorem 2) also hold true from the conclusions made by examining the experiment results.

All experimental code used to eliminate or disprove claims is included. Ans: **Yes**

Does this paper rely on one or more datasets? Ans: **Yes**

If yes, please complete the list below.

A motivation is given for why the experiments are conducted on the selected datasets. **Yes**, *we explained our motivation in detail in the data appendix in this document.*

All novel datasets introduced in this paper are included in a data appendix. **NA** No novel datasets are used.

All novel datasets introduced in this paper will be made publicly available upon publication of the paper with a license that allows free usage for research purposes. Ans: **NA**

All datasets drawn from the existing literature (potentially including authors' own previously published work) are accompanied by appropriate citations. Ans: **Yes**

All datasets drawn from the existing literature (potentially including authors' own previously published work) are publicly available. Ans: **Yes**

All datasets that are not publicly available are described in detail, with explanation why publicly available alternatives are not scientifically satisfying. Ans: **NA**: We have done all our experiments on publicly available datasets.

Does this paper include computational experiments? **Yes**

Any code required for pre-processing data is included in the appendix. Ans: **Yes** We have provided the pre-processing code in the code appendix zipped together with this supplementary material.

All source code required for conducting and analyzing the experiments is included in a code appendix. **Yes**

All source code required for conducting and analyzing the experiments will be made publicly available upon publication of the paper with a license that allows free usage for research purposes. **Yes** Once upon publication, we plan to release the code in the library python format so that its easier for researchers to build tools that use federated fine-tuning of transformer models and integrate it with their existing codebases.

All source code implementing new methods have comments detailing the implementation, with references to the paper where each step comes from. **Yes**

If an algorithm depends on randomness, then the method used for setting seeds is described in a way sufficient to allow replication of results. **Yes** All the details regarding the seed settings are described in the code appendix in the README as well as comments in the code.

This paper specifies the computing infrastructure used for running experiments (hardware and software), including GPU/CPU models; amount of memory; operating system; names and versions of relevant software libraries and frameworks. **Yes** Such information is detailed in the code appendix.

This paper formally describes evaluation metrics used and explains the motivation for choosing these metrics. **Partial** We haven't formally described the evaluation metrics that we have used (ROUGE L Score, BLEU-4 score), but we have cited their papers. Also we have provided the motivation to use these metrics in both supplementary material as well as main paper.

This paper states the number of algorithm runs used to compute each reported result. **Yes**

Analysis of experiments goes beyond single-dimensional summaries of performance (e.g., average; median) to include measures of variation, confidence, or other distributional information. Ans: **Yes** We did our experiments on multiple numbers of clients, datasets, models, and even client label configurations.

The significance of any improvement or decrease in performance is judged using appropriate statistical tests (e.g., Wilcoxon signed-rank). **Yes**, we perform and make our conclusions based on extensive experiments across multiple datasets, numbers of clients, and models.

This paper lists all final (hyper-)parameters used for each model/algorithm in the paper's experiments. **Yes**

This paper states the number and range of values tried per (hyper-) parameter during development of the paper, along with the criterion used for selecting the final parameter setting. **No**